RadioGraphics

From the Radiologic Pathology Archives[1]

Organization and Fibrosis as a Response to Lung Injury in Diffuse Alveolar Damage, Organizing Pneumonia, and Acute Fibrinous and Organizing Pneumonia[2]

Seth J. Kligerman, MD • Teri J. Franks, MD • Jeffrey R. Galvin, MD

TEACHING POINTS
See last page

Organization, characterized by fibroblast proliferation, is a common and nearly universal response to lung injury whether it is focal or diffuse. Despite the vast range of injurious agents, the lung's response to injury is quite limited, with a similar pattern of reaction seen radiologically and histologically regardless of the underlying cause. Although there is a tendency to divide organization into distinct entities, the underlying injury to the alveolar epithelial basement membrane is a uniting factor in these processes. This pattern of lung injury is seen in the organizing phase of diffuse alveolar damage, organizing pneumonia (OP), acute fibrinous and organizing pneumonia, and certain types of fibrotic lung disease. In addition, although organization can heal without significant injury, in some instances it progresses to fibrosis, which can be severe. When fibrosis due to organization is present, other histologic and imaging patterns, such as those seen in nonspecific interstitial pneumonia, can develop, reflecting that fibrosis can be a sequela of organization. This article reviews the histologic and radiologic findings of organization in lung injury due to diffuse alveolar damage, OP, and acute fibrinous and organizing pneumonia and helps radiologists understand that the histologic and radiologic findings depend on the degree of injury and the subsequent healing response.

Abbreviations: AFOP = acute fibrinous and organizing pneumonia, COP = cryptogenic organizing pneumonia, DAD = diffuse alveolar damage, GGO = ground-glass opacity, H-E = hematoxylin-eosin, NSIP = nonspecific interstitial pneumonia, OP = organizing pneumonia, UIP = usual interstitial pneumonia

RadioGraphics 2013; 33:1951–1975 • **Published online** 10.1148/rg.337130057 • **Content Codes:** CH CT

[1]Supported by the American Institute for Radiologic Pathology (AIRP), The Joint Pathology Center (JPC), and Uniformed Services University of the Health Sciences (USU).

[2]From the Departments of Diagnostic Radiology and Nuclear Medicine (Chest Imaging) (S.J.K., J.R.G.) and Internal Medicine (Pulmonary/Critical Care) (J.R.G.), University of Maryland School of Medicine, 22 S Greene St, Baltimore, MD 21201; Division of Pulmonary and Mediastinal Pathology, The Joint Pathology Center, Joint Task Force National Capital Region Medical, Silver Spring, Md (T.J.F.); and Department of Chest Imaging, American Institute for Radiologic Pathology, Silver Spring, Md (J.R.G.). Received August 15, 2013; accepted August 21. All authors have no financial relationships to disclose. **Address correspondence to** S.J.K. (e-mail: *skligerman@umm.edu*).

The views expressed in this article are those of the authors and do not reflect the official policy of the Department of Defense or the United States Government.

Introduction

Organization is a common and nearly universal response to injury in the lung, whether focal or diffuse. In most circumstances, the organization clears as part of the normal process of repair. However, in some instances, repair is self-reinforcing and leads to fibrosis.

Normal Lung Ultrastructure

Alveolar walls, composed of a capillary network with blood separated from air on both sides by only a thin layer of tissue, serve as the barrier between the environment and the interior of our bodies for the purpose of gas exchange (Fig 1). Ultrastructurally, the air-blood tissue barrier of the alveolar walls has three components: alveolar epithelial cells, a narrow interstitial space, and capillary endothelial cells (Fig 2). Nearly half of the interstitial space is composed solely of the fused basement membranes of epithelial and endothelial cells. Where the basement membranes are separated, the interstitial space contains elastic fibers, collagen fibrils, fibroblasts, and tissue macrophages (2). As the site for gas exchange, the lungs process an average of 10,000 L of air and 7000 L of blood per day. In addition to carrying beneficial constituents, air and blood have the potential to carry noxious environmental and endogenous agents to the lungs that may cause injury.

Lung Injury

Lung injury is associated with a myriad of causes such as infection, collagen-vascular disease, hypersensitivity processes, drug reaction, dust exposure, and toxic inhalation. Although the range of injurious agents is vast, the lung's response to injury is quite limited resulting in similar patterns of reaction seen radiologically and histologically regardless of the cause of injury (3). Organization, characterized by fibroblast proliferation, has long been recognized as an important pattern of response in lung injury (4,5) and is the result of damage to the air-blood tissue barrier of the alveolar walls (6).

Following injury, lung repair is a two-edged sword that may lead to resolution and return to normal lung architecture, or that may progress to irreversible fibrosis with complete loss of alveolar architecture (7). Injury may manifest as damage to alveolar epithelial cells, basement membranes, or capillary endothelial cells, and in the most severe injury, it may result in collapse of the collagen and elastic scaffold of the alveolar walls (7).

1.

2.

Figures 1, 2. Normal alveolar wall. **(1)** Photomicrograph (original magnification, ×600; hematoxylin-eosin [H-E] stain) shows the capillary network; however, the constituents of the alveolar wall cannot be resolved at light microscopy. **(2)** *A*, Electron photomicrograph (original magnification, ×2200; uranyl acetate stain) shows the capillary network, type I and type II pneumocytes (alveolar epithelial cells), and red blood cells *(RBC)* in the capillary lumens. *B,* Electron photomicrograph (original magnification, ×48,000; uranyl acetate stain) shows the thinnest portion of the tissue barrier between the alveolar space and the capillary lumen, which is composed of the cytoplasm of the type I pneumocyte, the fused basement membranes *(BM)* of the pneumocyte and the capillary endothelial cell, and the cytoplasm of the endothelial cell. (Fig 2, adapted and reprinted with permission from reference 1.)

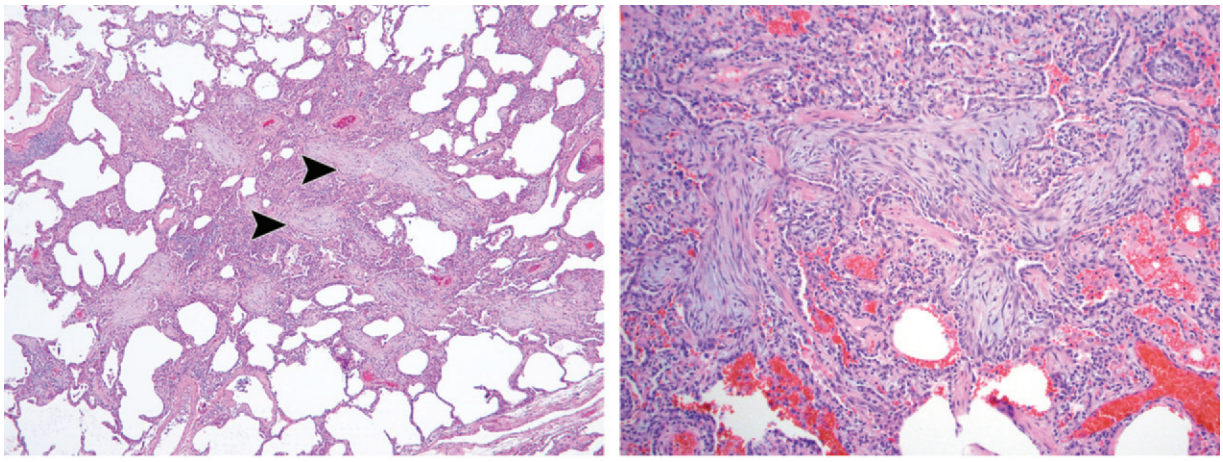

a. b.

Figure 3. Histologic pattern of OP. **(a)** Photomicrograph (original magnification, ×40; H-E stain) shows multiple plugs of organizing fibroblastic tissue (arrowheads). **(b)** Photomicrograph (original magnification, ×100; H-E stain) shows that the plugs are composed of spindle-shaped cells embedded in a pale-blue–staining matrix.

Teaching Point

The common result of injury is that a protein-rich exudate leaks from the barrier into the alveolar space and is associated with migration of fibroblasts from the interstitium, differentiation of some fibroblasts into myofibroblasts, and formation of organizing fibroblastic tissue (7).

The integrity of the epithelial and endothelial basement membranes is the key determinant of whether injured lung returns to normal or is replaced by fixed fibrous tissue (6). If the stimulus for injury is removed and the basement membranes are intact, then reepithelialization and reendothelialization occur, intraluminal fibroblastic tissue is remodeled into the interstitium (5,8) or is removed by the fibrinolytic system, and normal architecture is reestablished (6,7). If the stimulus for injury persists and the integrity of the basement membranes is lost, then alveoli collapse, their basement membranes fuse, fibroblast activation persists, and the self-reinforcing formation of organizing fibroblastic tissue progresses to fixed fibrosis (6,7).

Histologic Features of Organizing Fibroblastic Tissue

Organizing fibroblastic tissue, a histologic pattern termed organizing pneumonia (OP) or Masson bodies by pathologists, has a distinctive histologic appearance characterized by spindle-shaped fibroblasts and myofibroblasts (9) embedded in a pale-staining matrix (Fig 3). In response to injury, organizing fibroblastic tissue can be found microscopically in airspaces, in the interstitium, and in varying stages of incorporation from airspaces into the interstitium.

In a light and electron microscopy study of open lung biopsies and autopsy specimens from 373 individuals, Basset et al (5) describe this distribution of organizing fibroblastic tissue in detail and identify three patterns. First, intraluminal buds or plugs of organizing fibroblastic tissue partially fill affected alveoli and alveolar ducts. Variable amounts of inflammation and fibrosis occur in the buds, but fibrosis is not prominent. Second, obliterative change occurs with organizing fibroblastic tissue filling and obliterating whole lumens of alveoli, alveolar ducts, and respiratory or terminal bronchioles. There is loss of the epithelial lining in the affected areas. Variable inflammation and fibrosis are present in the areas of obliteration, but fibrosis is prominent. Third, mural incorporation is characterized by buds of fibroblastic tissue fused with nearby alveolar septa, alveolar ducts, or bronchiolar structures. The surface of the incorporated organizing fibroblastic tissue is reepithelialized. Fibrosis of the incorporated tissue is prominent, and along with obliterative change causes remodeling of the lung parenchyma (Fig 4). Studies by Auerbach et al (4), Fukuda et al (11), Myers and Katzenstein (8), and Peyrol et al (12) describe similar patterns of organizing fibroblastic tissue in lung injury.

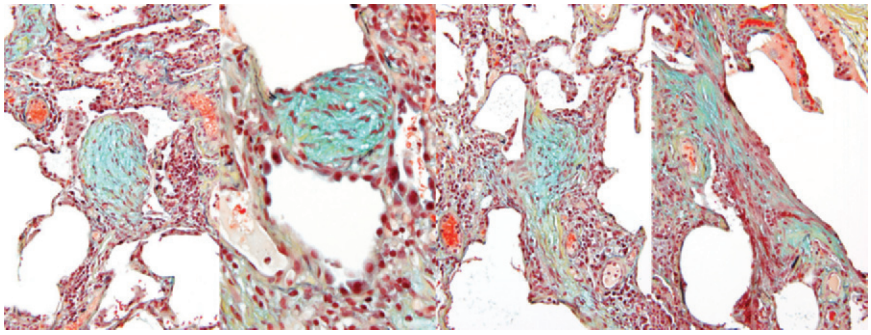

Figure 4. Incorporation of intraalveolar organization. OP is evidenced by intraalveolar plugs of organizing fibroblastic tissue, which stain green in this collage of four images. Photomicrographs (original magnifications from left to right: ×100, ×200, ×100, and ×100; Movat pentachrome stain) show OP that appears initially as rounded plugs within the alveolar spaces (far left). As clearance begins, the plugs abut alveolar walls and become epithelialized by an overgrowth of type II pneumocytes (middle left). Plugs are then incorporated into the alveolar walls (middle right). Over time, they become relatively flattened and collagenized (far right) but result in thickening of the alveolar walls. (Reprinted, with permission, from reference 10.)

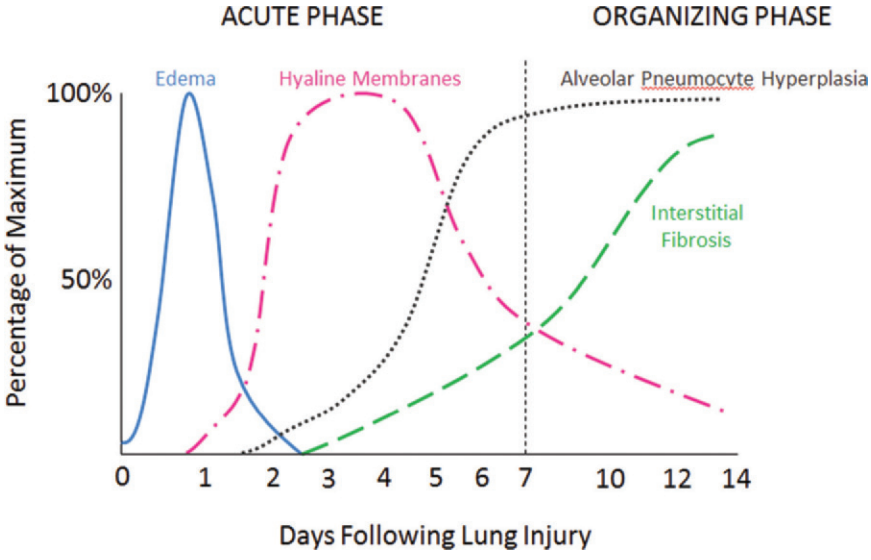

Figure 5. Time course of histologic events in DAD. The graph shows the chronologic appearance of the histologic features of DAD. (Adapted, with permission, from reference 3.)

Organizing fibroblastic tissue is commonly thought to occur predominantly in acute and subacute lung injury, namely in diffuse alveolar damage (DAD) and cryptogenic organizing pneumonia (COP). However, it is a histologic feature in a wide range of interstitial lung disorders such as collagen-vascular disease; hypersensitivity pneumonitis; chronic eosinophilic pneumonia; pulmonary Langerhans cell histiocytosis; pulmonary sarcoidosis; pneumoconioses; lymphangioleiomyomatosis; drug-, toxin-, and radiation-induced lung injury; and idiopathic pulmonary fibrosis (5). Precise identification of the distribution of organizing fibroblastic tissue in the histologic section is essential for accurate diagnosis. In addition, many studies have demonstrated that organizing fibroblastic tissue is a pathway to lung fibrosis (4,5,8,11,12). The following sections review the most common settings of organization as a response to lung injury.

Histologic and Radiologic Findings of DAD

DAD is a nonspecific reaction of the lung to a wide range of toxic insults including those due to infection, drugs, sepsis, shock, aspiration, toxic inhalation, toxic ingestants, exacerbation of idiopathic pulmonary fibrosis, and a wide variety of miscellaneous sources (3). In the absence of an identifiable cause, DAD may be idiopathic, in

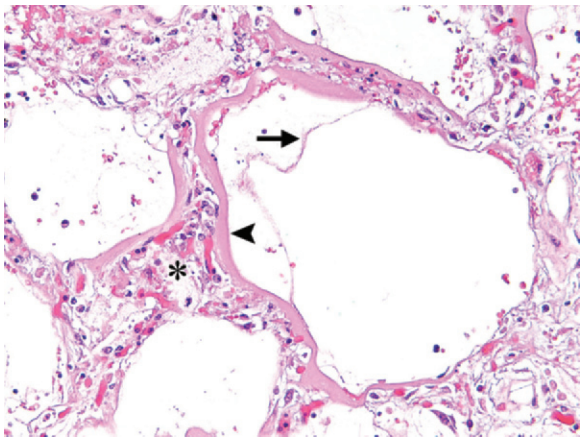

Figure 6. Acute phase DAD. Photomicrograph (original magnification, ×200; H-E stain) shows characteristic hyaline membranes (arrowhead) and alveolar wall edema (*) in acute phase DAD. Capillary leak has resulted in amorphous eosinophilic edema fluid in alveolar spaces (arrow).

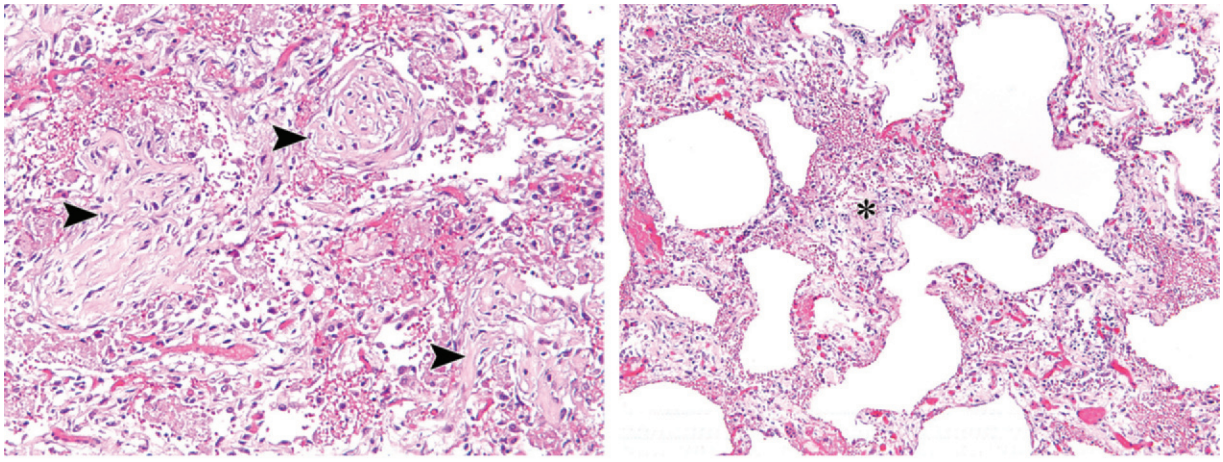

a. b.

Figure 7. Organizing phase DAD. Photomicrographs (original magnifications, ×320 **[a]** and ×100 **[b]**; H-E stain) in the same patient show organizing fibroblastic tissue as plugs within the alveolar spaces (arrowheads in **a**) and diffusely involving the interstitium (* in **b**).

which case the clinical diagnosis of acute interstitial pneumonia, previously termed *Hamman-Rich syndrome*, may be applied (13). *DAD* also is the descriptive term used by pathologists to encompass the series of events seen histologically following acute lung injury from any cause.

The histologic appearance of DAD depends on the time from the initial lung injury to lung biopsy, which typically is divided into two phases (Fig 5). From the initial injury through day 7, acute or early phase DAD is characterized histologically by the presence of hyaline membranes and edema of the alveolar walls (Fig 6). Hyaline membranes are homogeneous eosinophilic material composed of cellular debris, plasma proteins, and surfactant plastered against alveolar ducts and alveolar walls (11,14). Alveolar epithelial cells throughout the affected parenchyma are diffusely damaged resulting in exposure of the epithelial basement membranes as the alveolar walls become denuded of damaged epithelial lining cells.

After the first week, the organizing phase of DAD predominates and is characterized by organizing fibroblastic tissue and fibrosis (Fig 7) (3). In response to injury, organizing fibroblastic tissue is present in both alveolar spaces and in the interstitium, which can resolve or progress to fibrosis. Alveolar collapse can be seen in both the acute and organizing phases and accounts for the striking volume loss seen in patients with DAD (Fig 8) (11,15–17). It is important to note that the two phases of DAD shown in the graph in Figure 5 are not strictly sequential, that a great deal of overlap exists between the two phases with many histologic features occurring in tandem, and that the timing of the appearance of the various histologic findings is a rough approximation. The term *diffuse* in DAD is confusing because it suggests that the

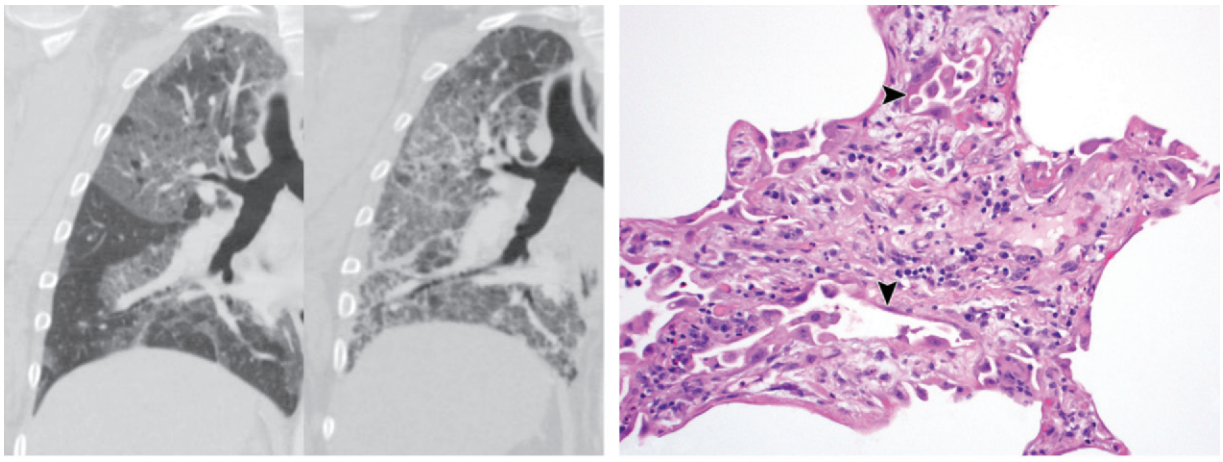

a. b.

Figure 8. Organizing and fibrotic phase DAD in a 56-year-old man. **(a)** Coronal reconstructed images from axial CT demonstrate large geographic regions of consolidation at initial imaging (left) that progressed to near-total opacification 2 weeks later (right). Volume loss is confirmed by elevation of the diaphragm. **(b)** Photomicrograph (original magnification, ×320; H-E stain) shows the collapsed alveoli (arrowheads), the major contribution to volume loss, in an alveolar wall markedly widened by organizing fibroblastic tissue.

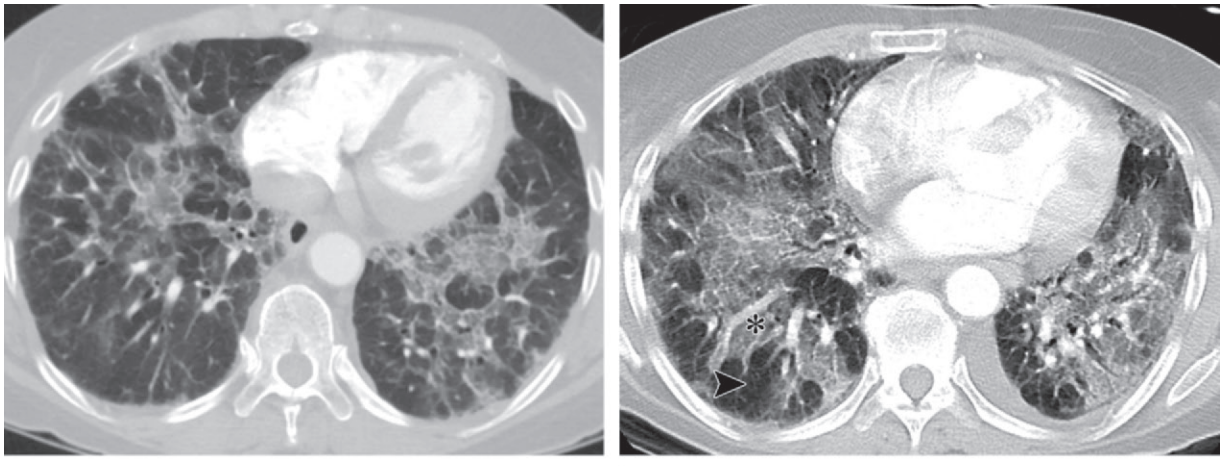

a. b.

Figure 9. Geographic distribution and septal thickening in DAD. **(a)** Axial CT image through the lower lobes demonstrates a geographic distribution of consolidation and ground-glass opacity (GGO). **(b)** In an axial CT image obtained 10 days after **a,** widespread consolidation is present with a clear demarcation between the involved lung (*) and the spared lobules (arrowhead). **(c)** Photomicrograph (original magnification, ×40; H-E stain) shows a fibrotic interlobular septum (*) separating areas of diffusely involved lung (right) from areas of less-involved lung (left). Microscopically, evidence of less severe lung injury is present even in the areas of radiologic sparing seen in **b**.

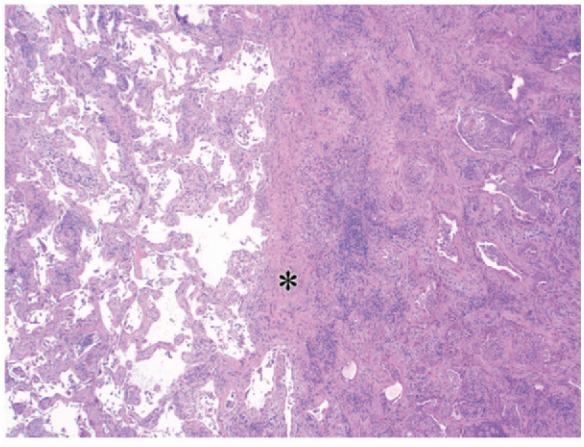

c.

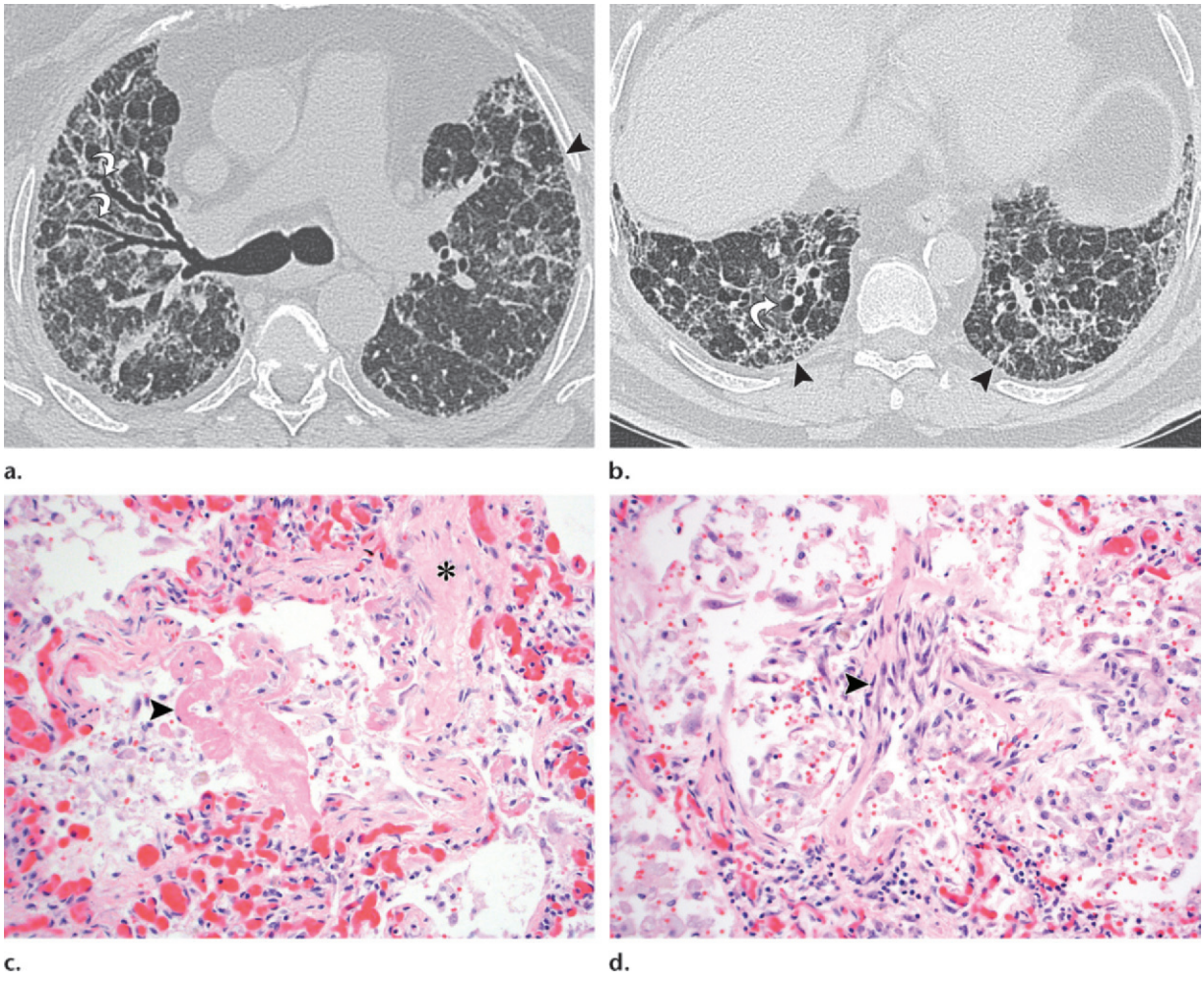

Figure 10. Organizing and fibrotic phase DAD in a 76-year-old man. **(a, b)** Axial thin-section CT images obtained through the upper **(a)** and lower **(b)** lobes demonstrate traction bronchiectasis (arrows) and widespread reticulation (arrowheads) with focal areas of sparing. The fibrotic phase of DAD predominates in this patient histologically. **(c)** In addition to interstitial fibrosis (*), this photomicrograph (original magnification ×200; H-E stain) shows a hyaline membrane (arrowhead) within an airspace. **(d)** Photomicrograph (original magnification ×200; H-E stain) shows organizing fibroblastic tissue (arrowhead) within an airspace.

lung is diffusely involved. However, the term is intended to convey the diffuse involvement of all constituents of the alveolar wall—the alveolar epithelium, basement membranes, and capillary endothelium (3). Thus, DAD may involve the entire lung but often demonstrates areas of sparing both histologically and at imaging (Fig 9).

Teaching Point

At imaging, the acute phase of DAD manifests as relatively diffuse but patchy GGO with areas of consolidation and septal thickening (Figs 8, 9). These findings reflect a combination of airspace exudates, interstitial edema, inflammation, and alveolar collapse that usually is most pronounced in the dependent portion of the lungs (18,19). Alveolar collapse also is promoted by external compression from the surrounding mediastinal and abdominal structures (19,20). Focal areas of spared, normal-attenuation, secondary lobules adjacent to the involved lung are a common finding and create a geographic appearance (Fig 9) (10,21,22). Traction bronchiectasis is absent or very mild in this phase and usually coincides with a transition to the organizing phase of the disease (22).

Histologic organization and subsequent fibrosis are mirrored by the CT findings. Dependent predominant GGO and consolidation likely represent a combination of lung organization and alveolar collapse. As the lung injury progresses, findings of fibrosis that include reticulation, traction bronchiectasis, and bronchiolectasis rapidly develop (Fig 10) (10,20,21,23). These findings are associated with a decreased likelihood of survival that varies

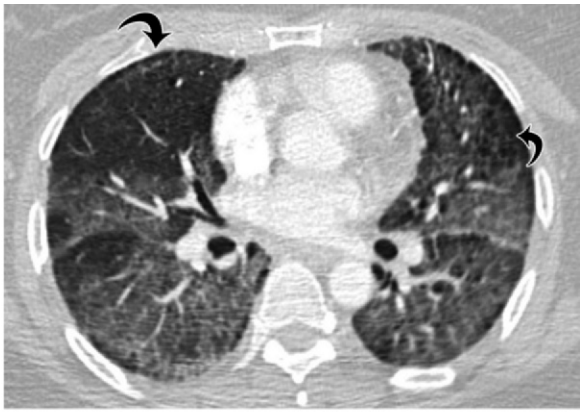

a.

b.

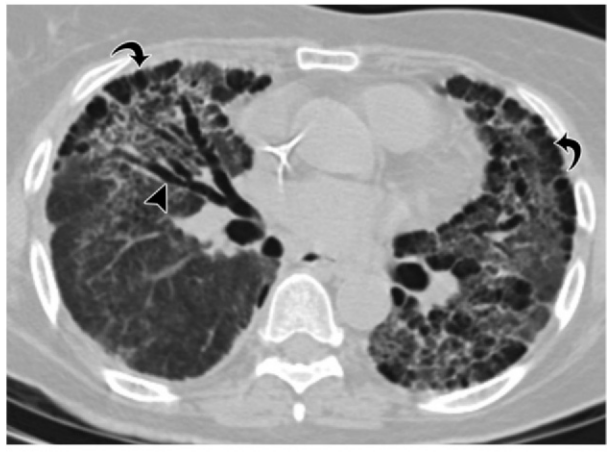

c.

Figure 11. Atypical pattern of fibrosis secondary to DAD. **(a)** Axial CT image at the level of the right middle lobe in a 36-year-old woman with worsening shortness of breath demonstrates basilar-predominant GGO. Small subpleural cysts are seen due to underlying paraseptal emphysema (arrows). **(b)** CT image at the same level 4 days later shows diffuse GGO with more dependent consolidation in the right lower lobe. Bronchiectasis (arrowhead) has developed, and the cystic spaces (arrows) have enlarged. A transbronchial biopsy confirmed DAD. **(c)** CT image obtained 9 months after **a** shows a bizarre pattern of anterior-predominant fibrosis that is most severe in the middle lung zone. Bronchiectasis (arrowhead) has progressed, and subpleural (arrows) and parenchymal cystic changes are prevalent.

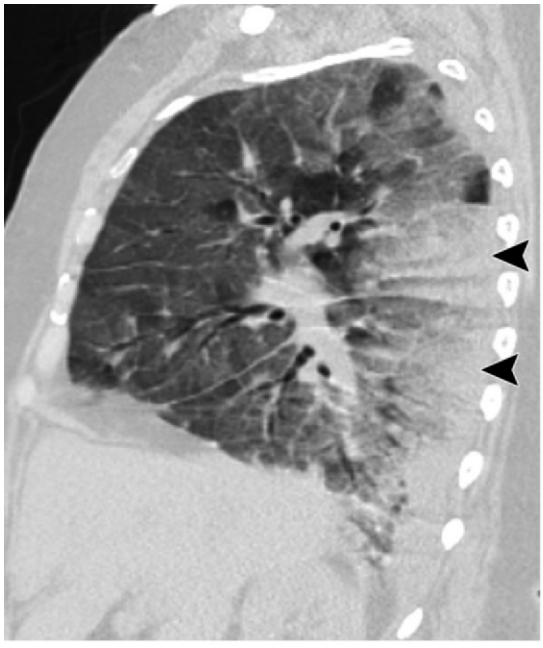

a.

b.

Figure 12. Change in the distribution of DAD over time. **(a)** Sagittal CT image obtained in a 34-year-old man during the acute phase of acute respiratory distress syndrome shows diffuse GGO, septal thickening, and dependent consolidation (arrowheads). **(b)** Sagittal CT image obtained 10 weeks after **a** shows resolution of the dependent consolidation. However, fibrosis (arrows) has developed in the anterior portion of the lungs, which showed only mild involvement during the acute phase.

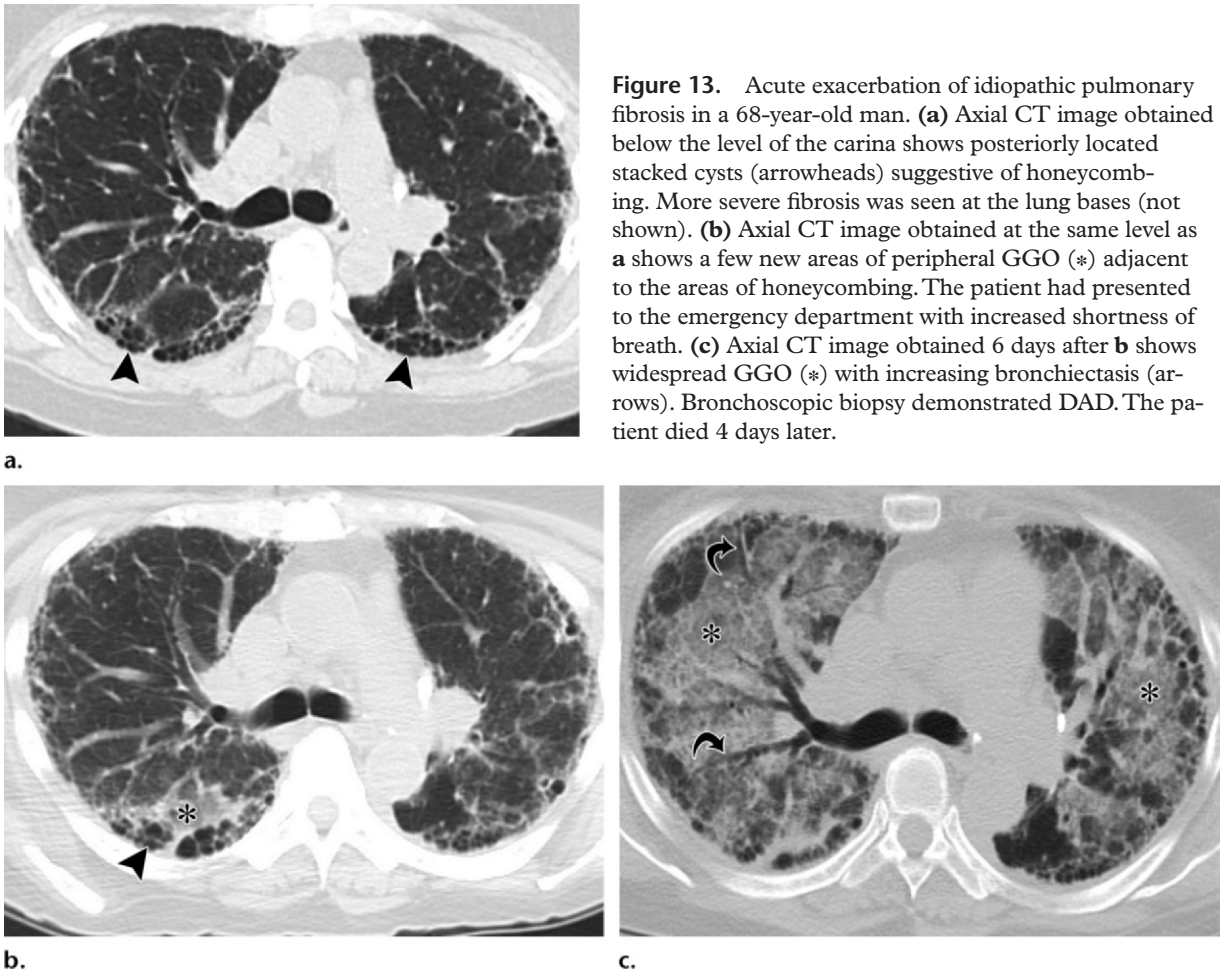

Figure 13. Acute exacerbation of idiopathic pulmonary fibrosis in a 68-year-old man. **(a)** Axial CT image obtained below the level of the carina shows posteriorly located stacked cysts (arrowheads) suggestive of honeycombing. More severe fibrosis was seen at the lung bases (not shown). **(b)** Axial CT image obtained at the same level as **a** shows a few new areas of peripheral GGO (*) adjacent to the areas of honeycombing. The patient had presented to the emergency department with increased shortness of breath. **(c)** Axial CT image obtained 6 days after **b** shows widespread GGO (*) with increasing bronchiectasis (arrows). Bronchoscopic biopsy demonstrated DAD. The patient died 4 days later.

from 35% to 50% (14,23–25). If a patient does survive, consolidation and GGO slowly improve.

Although CT findings can return to normal in some patients, between 38% and 85% of patients have residual fibrosis that can be extensive and debilitating (Fig 11) (20,26–30). Patients typically have an atypical pattern of fibrosis that involves less than 25% of the lung (26,27) and is most pronounced in the anterior nondependent portions of the lung (Fig 12) (18,21,23,27). The anterior location of the fibrosis may be related to barotrauma due to mechanical ventilation or oxygen toxicity, whereas the dependent lung is protected by collapse (29).

The limited extent of residual fibrosis, compared with the extensive parenchymal involvement seen in the acute and organizing phases of DAD, suggests that a normal reparative healing response has occurred, with reorganization of the damaged epithelial basement membranes and re-expansion of the alveoli. Imaging findings of anterior-predominant reticulation, bronchiectasis, and cystic spaces in combination with basilar sparing are helpful to making the diagnosis. Prior imaging studies that document a typical progression from the acute to the organizing phase of DAD add further certainty. Other helpful clues include a tracheostomy or a deformity in the anterior tracheal wall suggestive of prior tracheostomy.

An association between organizing lung injury and usual interstitial pneumonia (UIP) was described as early as 1973 and has been confirmed in many studies (31,32). This association is well documented in the setting of an acute exacerbation of UIP. This association, also referred to as an accelerated phase, occurs when histologic findings of DAD, or less commonly of OP, are superimposed on underlying UIP, which can lead to rapid clinical deterioration (33–37). In the setting of acute lung injury superimposed on a background of pulmonary fibrosis, 75%–86% mortality has been reported (34,36,37). The radiologic findings will mirror the histologic findings, with dependent predominant GGO and consolidation superimposed on a background pattern of UIP (Fig 13) (34,37). As the injury continues to organize, traction bronchiectasis and reticulation increase. Similar to DAD, some of the abnormality

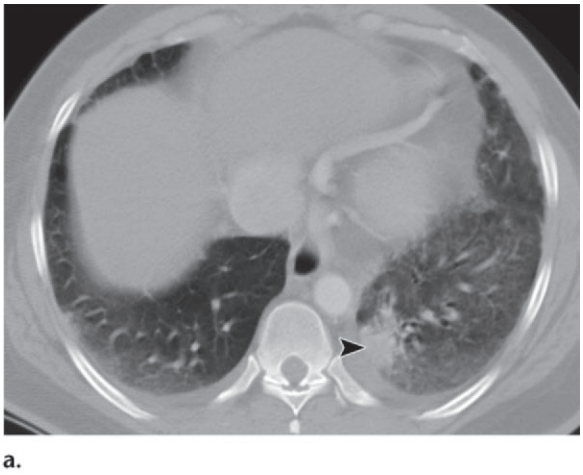

a.

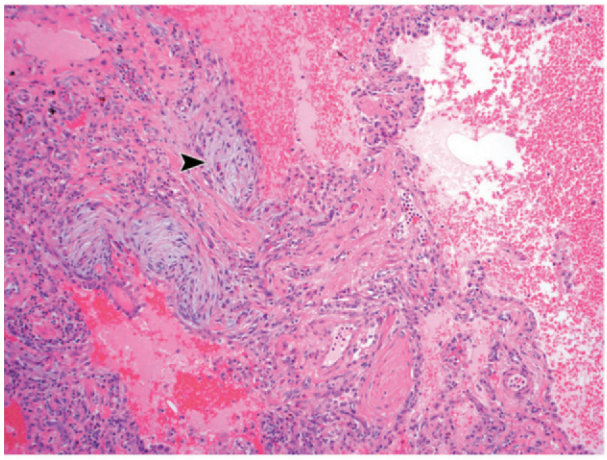

b.

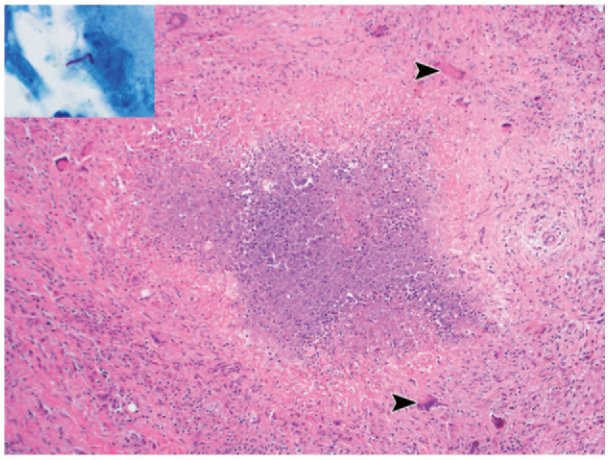

c.

Figure 14. OP at the periphery of a granuloma. **(a)** Axial CT image demonstrates a nodule in the posterior basal segment of the left lower lobe (arrowhead) with surrounding GGO. **(b)** Photomicrograph (original magnification, ×100; H-E stain) shows plugs of organizing fibroblastic tissue (arrowhead) at the margin of the nodule. **(c)** Photomicrograph (original magnification, ×100; H-E stain) of the nodule shows a necrotizing granuloma surrounded by multiple multinucleated giant cells (arrowheads). Inset photomicrograph (original magnification, ×1000; Ziehl Neelsen stain) shows an acid-fast bacillus in one of the multinucleated giant cells.

can resolve if the patient survives, although fibrosis may progress after each acute exacerbation. The cause of an acute exacerbation is unclear in most cases, although it has been reported after lung biopsy and bronchiolar lavage (34).

Basement membrane damage is a common finding at electron microscopy in patients with UIP even in the absence of an acute exacerbation. The relationship between UIP and the organization that occurs in response to acute or subacute lung injury is not entirely understood. However, the common histologic findings suggest that lung repair mechanisms may be partially responsible.

Histologic and Radiologic Findings of OP

The histologic response known as OP was first recognized during the early part of the 20th century in patients with "unresolved" pneumococcal pneumonia. At that time, OP was identified as a distinct pathologic response to pulmonary infection during which intraalveolar exudates were transformed into connective tissue (38). *OP* is a term used by pathologists to describe a histologic pattern that is a nonspecific response to lung injury. As a histologic pattern, OP is characterized by organizing fibroblastic plugs of tissue composed of spindle-shaped cells in a pale-staining matrix (Fig 3). Depending on the location within the airspaces where they form, these plugs may

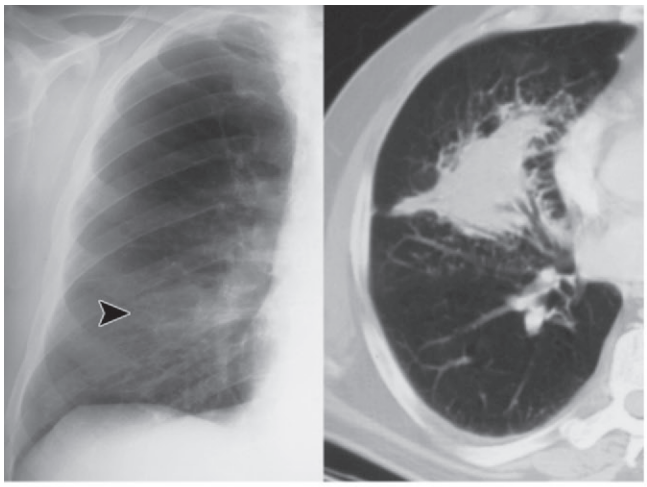

a.

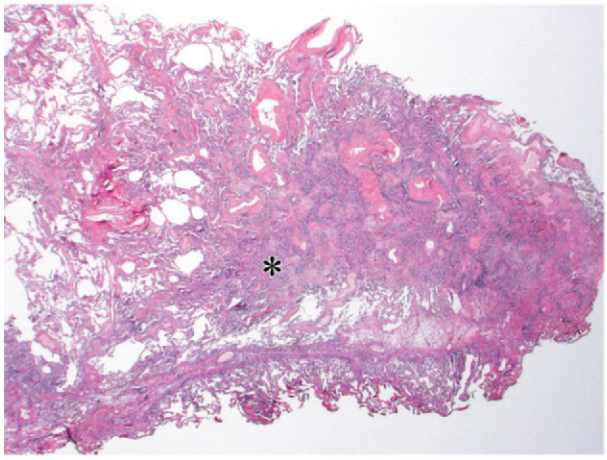

b.

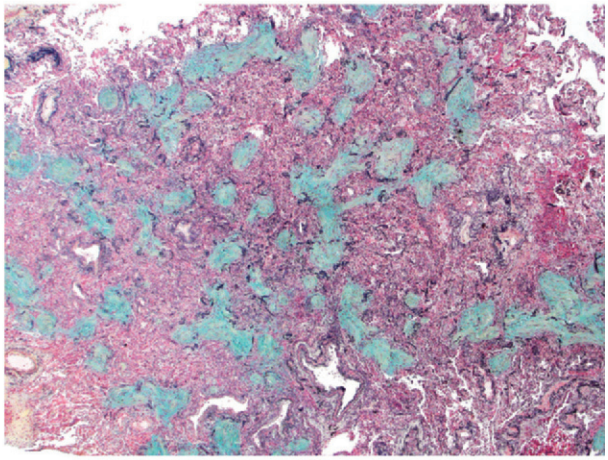

c.

Figure 15. OP in a 69-year-old man. **(a)** Radiograph (left) shows a focal area of consolidation in the right perihilar region (arrowhead). CT image (right) through the inferior portion of the right lung reveals peribronchial consolidation in the middle lobe. **(b)** Photomicrograph (original magnification, ×12.5; H-E stain) shows an ill-defined parenchymal nodule (*). **(c)** Photomicrograph (original magnification, ×40; Movat pentachrome stain) shows that the nodule is composed of variably shaped plugs of organizing fibroblastic tissue (stained green) within the alveolar spaces.

be round, oval, elongated, dumbbell-shaped, branching, or serpiginous.

Teaching Point

The clinical significance of a histologic finding of OP varies. The finding may be of little clinical significance, such as in the case of focal areas of OP that surround a granuloma or malignancy (Fig 14). In addition, OP can be a minor component of diffuse lung disease such as hypersensitivity pneumonitis, eosinophilic pneumonia, or pulmonary Langerhans cell histiocytosis (3). On the other hand, the pattern may be widespread and may be the cause of the underlying clinical illness.

Although OP is most commonly a sequela of infection, there are numerous other causes including collagen-vascular disease, immunologic disorders, drug reaction, aspiration, toxic inhalation, radiation, organ transplantation, and miscellaneous causes (39–41). In the absence of an identifiable cause, OP can be considered idiopathic, and the clinical diagnosis of COP may be appropriate (42). There are no clinical, radiologic, or histologic features that reliably distinguish COP from secondary OP or distinguish among the secondary causes because the response to lung injury is the same (39–44). At CT, numerous imaging patterns are associated with OP. These findings are most often diffuse, but focal or unilateral abnormalities do occur.

Unilateral Patterns of OP at Imaging

While diffuse patterns predominate, in 10%–38% of patients OP can present as a solitary pulmonary nodule (Fig 14), a focal area of consolidation (Fig 15), and/or focal GGO (40,45–47).

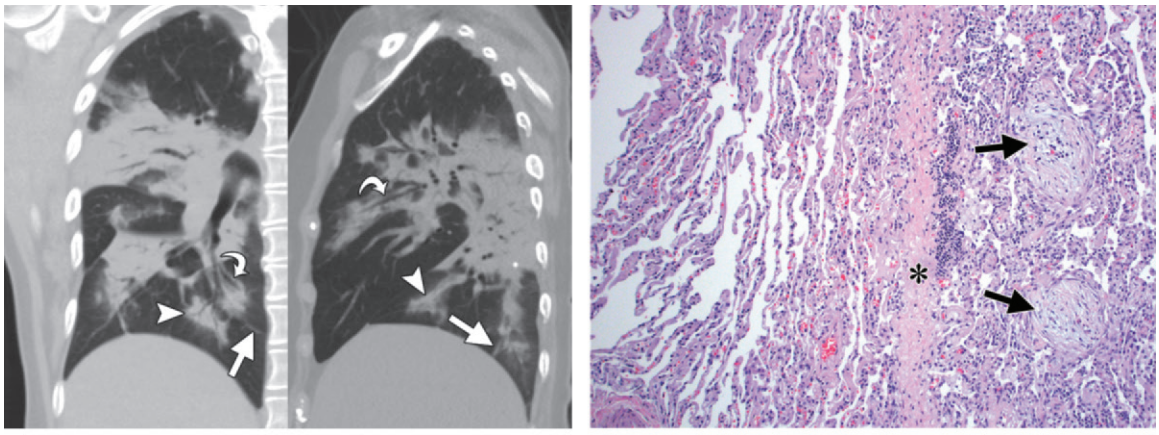

a. b.

Figure 16. OP in a 58-year-old woman. **(a)** Coronal (left) and sagittal (right) reconstructed CT images of the right lung reveal a striking peribronchial distribution of consolidation (arrowheads). Some of the airways are mildly bronchiectatic (curved arrows). Numerous faint septal lines (straight arrows) are identified within the regions of GGO. **(b)** Photomicrograph (original magnification, ×100; H-E stain) shows a fibrotic interlobular septum (*) that correlates with the septal thickening seen at imaging. Plugs of organizing fibroblastic tissue within the alveolar spaces (arrows) and mildly widened alveolar walls due to collagen deposition, mild infiltrates of chronic inflammatory cells, and type 2 pneumocyte hyperplasia are the histologic findings underlying the GGO. To the left of the interlobular septum, the lung parenchyma is relatively normal.

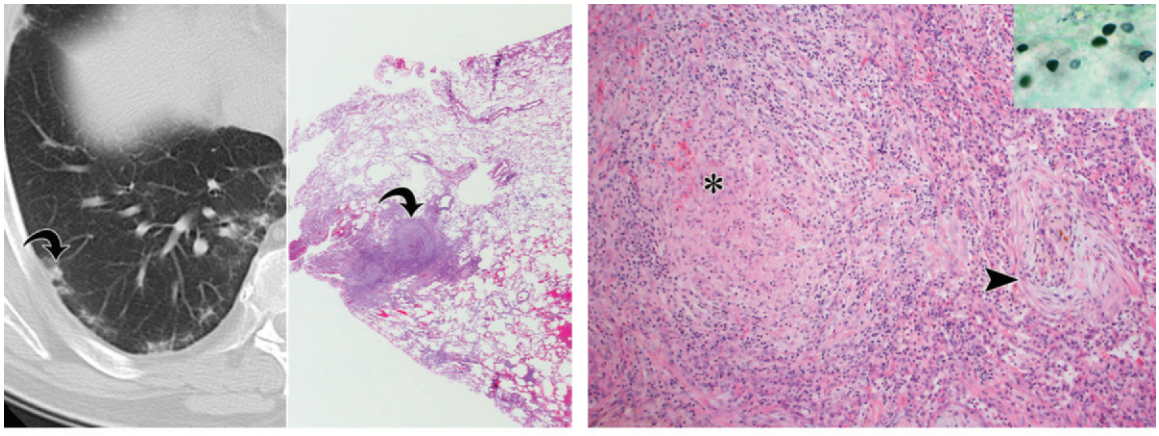

a. b.

Figure 17. OP from *Pneumocystis* infection. **(a)** CT image through the right lower lobe (left) reveals an irregular line of unilateral peribronchiolar consolidation with an ill-defined nodule (arrow) abutting the pleura. Photomicrograph (right) (original magnification, ×12.5; H-E stain) demonstrates the nodule. **(b)** Photomicrograph (original magnification, ×100; H-E stain) shows that the nodules are composed of a combination of necrotizing granulomas (*) and plugs of organizing fibroblastic tissue (arrowhead). Inset photomicrograph (original magnification, ×1000; Gomori methenamine silver stain) shows *Pneumocystis jirovecii* within the granulomas.

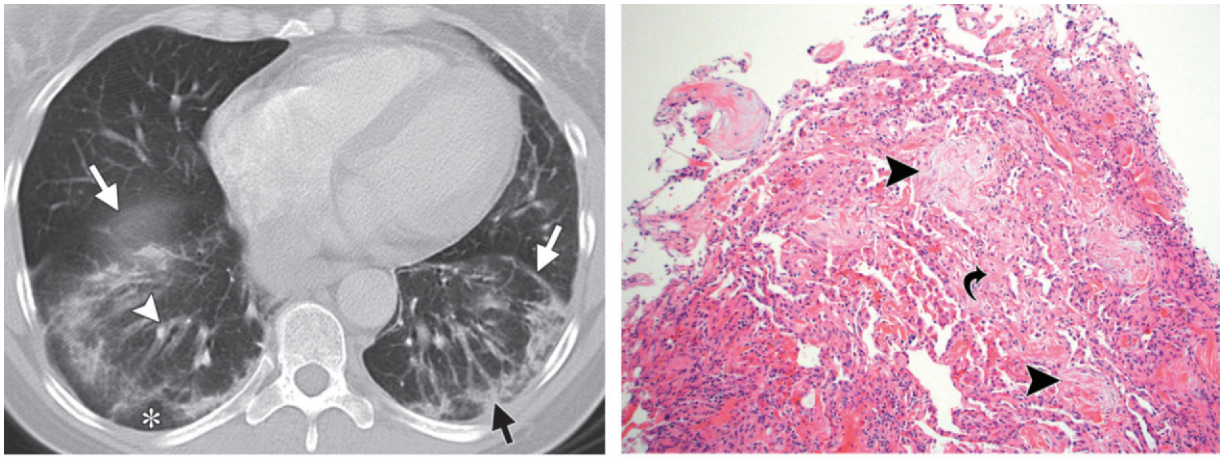

a. b.

Figure 18. OP in a 51-year-old woman with a history of rheumatoid arthritis and dyspnea. **(a)** Axial CT image just above the level of the diaphragm reveals bandlike areas of peripheral (black arrow) and peribronchial (arrowhead) consolidation in the periphery of both lower lobes with peripheral sparing (*). Volume loss in the lower lobes is indicated by posterior displacement of the major fissures (white arrows). **(b)** Photomicrograph (original magnification, ×100; H-E stain) from a transbronchial biopsy shows multiple plugs of organizing fibroblastic tissue (arrowheads). Focally the alveolar walls are widened because of fibrosis (arrow).

Although unilateral parenchymal consolidation is a nonspecific finding, consolidation with a peribronchial distribution associated with bronchiectasis or architectural distortion is a finding that can help to differentiate OP from other causes such as acute pneumonia or pulmonary hemorrhage (Fig 16). Nodules secondary to OP also can be unilateral and may have a wide range of imaging appearances. Nodules can vary in size, but they often are peribronchial or peribronchiolar and may be associated with areas of consolidation or GGO (Fig 17).

In some instances, OP manifests as a solitary spiculated or lobulated nodule that mimics a lung cancer. In addition, it also can manifest as a nonresolving ground-glass nodule with internal air bronchograms that can mimic various subtypes of adenocarcinoma. Unfortunately, even if a biopsy confirms OP in a solitary lesion, surgical excision is still sometimes necessary because it is not uncommon for OP to occur adjacent to a lung malignancy (48).

Diffuse Patterns of OP at Imaging

Although focal disease can occur, most patients with COP and secondary OP present with various patterns of diffuse parenchymal abnormality. While some patterns are highly suggestive of a diagnosis of OP, in many instances the findings are nonspecific. The dominant finding in OP is the presence of bilateral consolidation, which occurs in 80%–95% of cases (21,49,50). Although consolidation itself is a nonspecific finding, bilateral consolidation that is predominantly peripheral or peribronchial is commonly seen with OP (Fig 18) (43,51,52). Sparing of the subpleural portion of

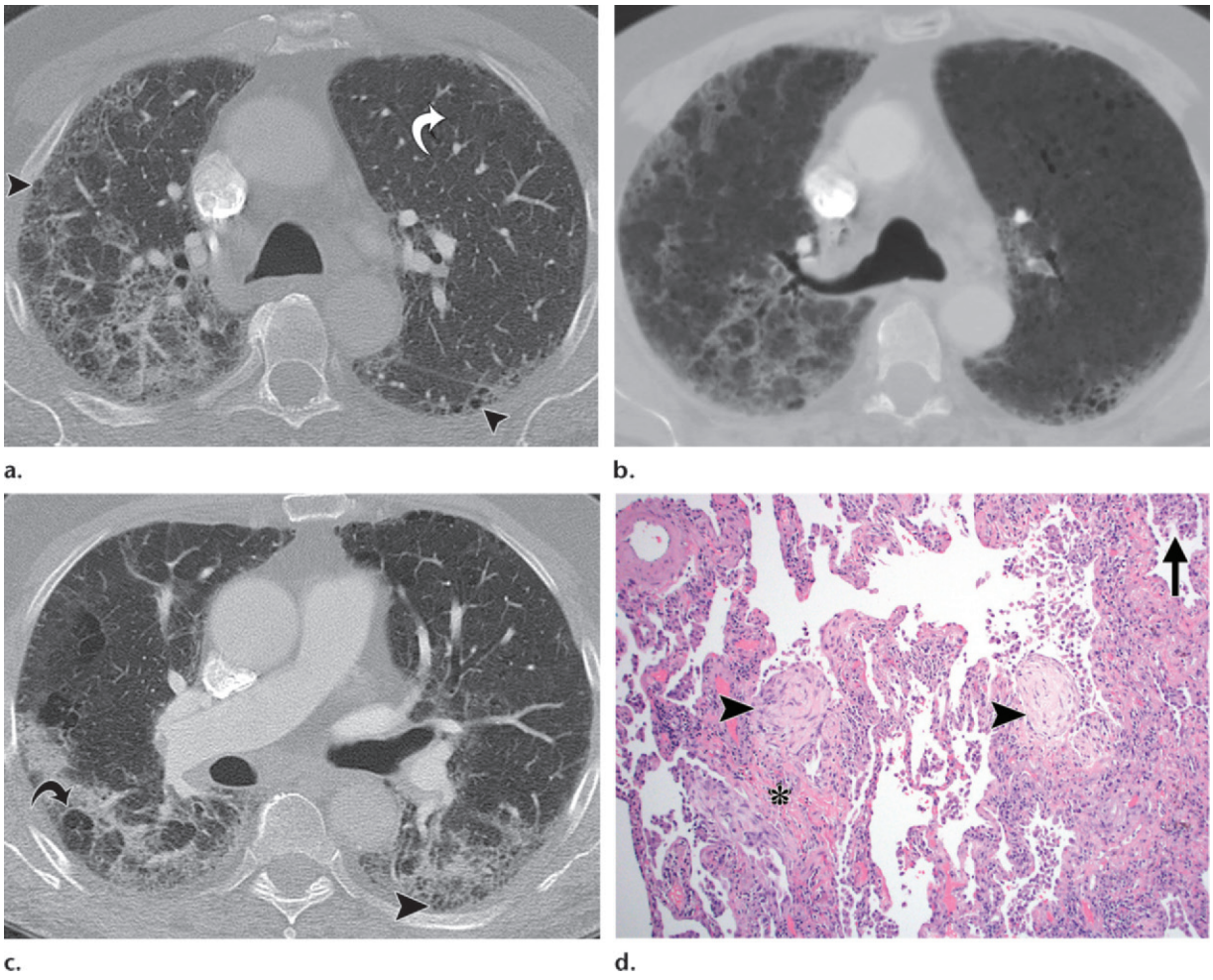

Figure 19. OP in a 62-year-old male cigarette smoker with progressive dyspnea. **(a)** Axial CT image through the upper lobes demonstrates patchy consolidation in the posterior aspect of the right upper lobe. Numerous 2–3-mm cysts are noted in the posterior aspect and the periphery of the left and right upper lobes (arrowheads). Focal areas of low attenuation without walls are identified in the anterior aspect of the left upper lobe (arrow). **(b)** Low-attenuation areas are better appreciated as a diffuse process on a 6-mm-thick minimum intensity projection image at the same level. **(c)** Axial CT image obtained just caudal to the carina demonstrates bandlike areas of peripheral consolidation in the dependent portions of both lungs. Subpleural curvilinear opacities bordering the secondary lobule (arrow) create what is sometimes referred to as a perilobular pattern. Small cysts are once again noted within the areas of consolidation (arrowhead). **(d)** Photomicrograph (original magnification, ×100; H-E stain) shows airspace enlargement consistent with emphysema associated with thick fibrotic alveolar walls (*), respiratory bronchiolitis ("smokers' macrophages") (arrow), and plugs of organizing fibroblastic tissue partially incorporated into the alveolar walls (arrowheads).

the lung along with thickened septa can create a geographic pattern where more heavily involved lung lies directly adjacent to less-involved or normal parenchyma (Fig 19). These areas of normal lung interspersed in areas of extensive parenchymal abnormality occur because of the zonal nature of the injury to the alveolar epithelium, which is mirrored at histologic analysis (12).

Perilobular opacities, which often are subpleural, are a common finding in OP and are seen in up to 57% of patients (50,53). They appear as poorly defined curvilinear or polygonal opacities that border the secondary pulmonary lobule and may represent a combination of dilated septal lymphatics and septal fibrosis (Fig 20).

Migratory opacities are reported in 11%–24% of cases of OP (43,49,51). However, migratory opacities are a nonspecific finding in numerous

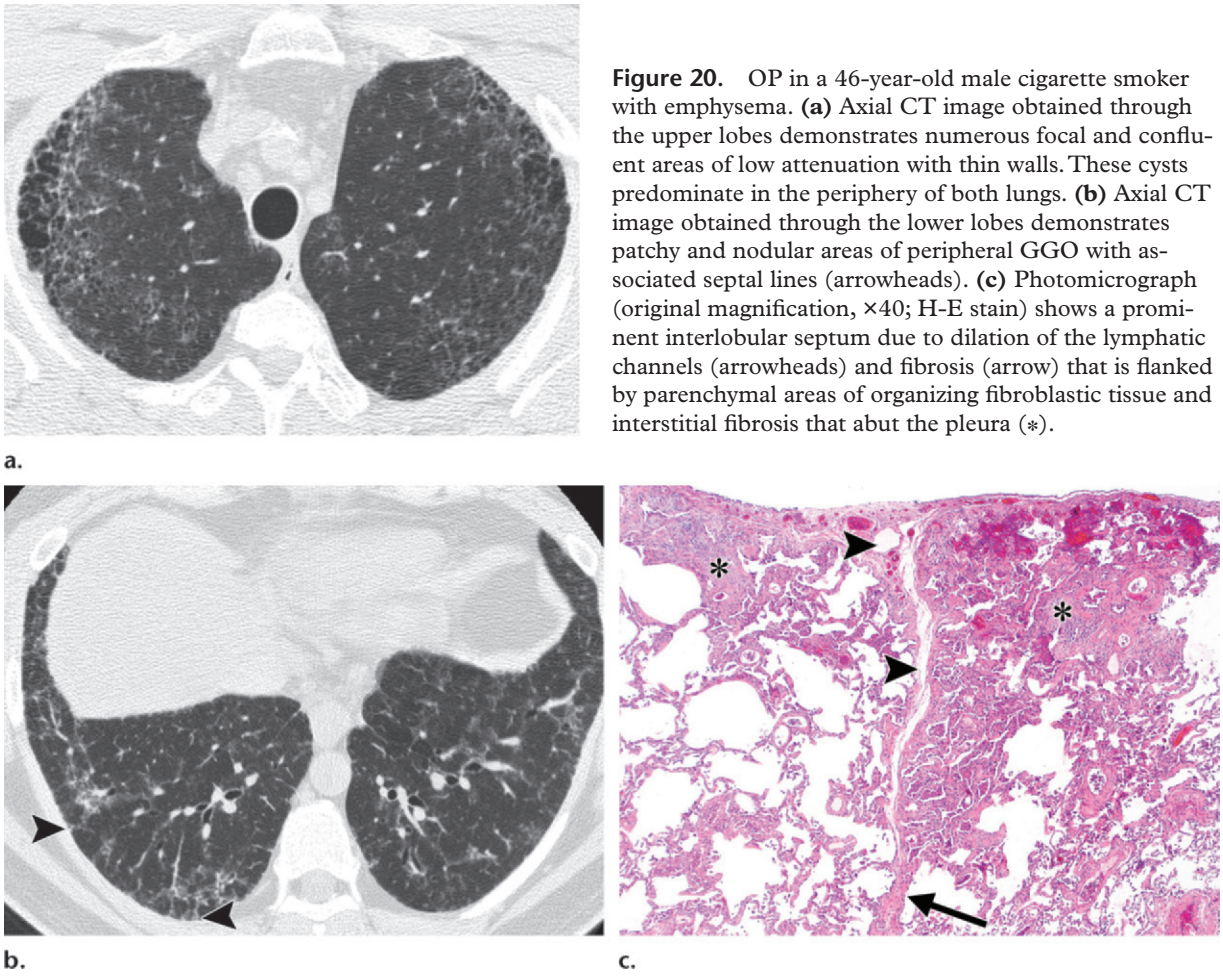

Figure 20. OP in a 46-year-old male cigarette smoker with emphysema. **(a)** Axial CT image obtained through the upper lobes demonstrates numerous focal and confluent areas of low attenuation with thin walls. These cysts predominate in the periphery of both lungs. **(b)** Axial CT image obtained through the lower lobes demonstrates patchy and nodular areas of peripheral GGO with associated septal lines (arrowheads). **(c)** Photomicrograph (original magnification, ×40; H-E stain) shows a prominent interlobular septum due to dilation of the lymphatic channels (arrowheads) and fibrosis (arrow) that is flanked by parenchymal areas of organizing fibroblastic tissue and interstitial fibrosis that abut the pleura (*).

Figure 21. CT findings of COP. Axial image obtained in a 56-year-old woman shows multiple findings classically associated with OP, including the reverse halo sign (arrowhead) and the atoll sign (straight arrows). A 9-mm nodule is seen in the right middle lobe with an internal air bronchogram (curved arrow). Although this type of nodule can be seen with various pathologic processes, additional CT findings of OP can help confirm the diagnosis.

pathologic conditions, including pulmonary eosinophilia, pulmonary hemorrhage, and recurrent infection or aspiration (54). The "reverse halo" sign is a CT finding defined by the presence of a focal area of GGO surrounded by a ring of denser consolidation (Fig 21). When this surrounding ring is incomplete, it is referred to as an "atoll" sign. Although initially thought to be a specific sign of OP, it can be seen in a variety of infections, noninfectious granulomatous abnormalities, and even adenocarcinoma in situ (55,56).

OP also can manifest with peribronchial or peribronchiolar nodules of various sizes and the location of these nodules around the airways suggests that this is often the initial site of injury (8). These nodules usually are peripheral and often contain internal air bronchograms when larger in size (Fig 22) (57). These nodules often coexist with other parenchymal findings of OP that

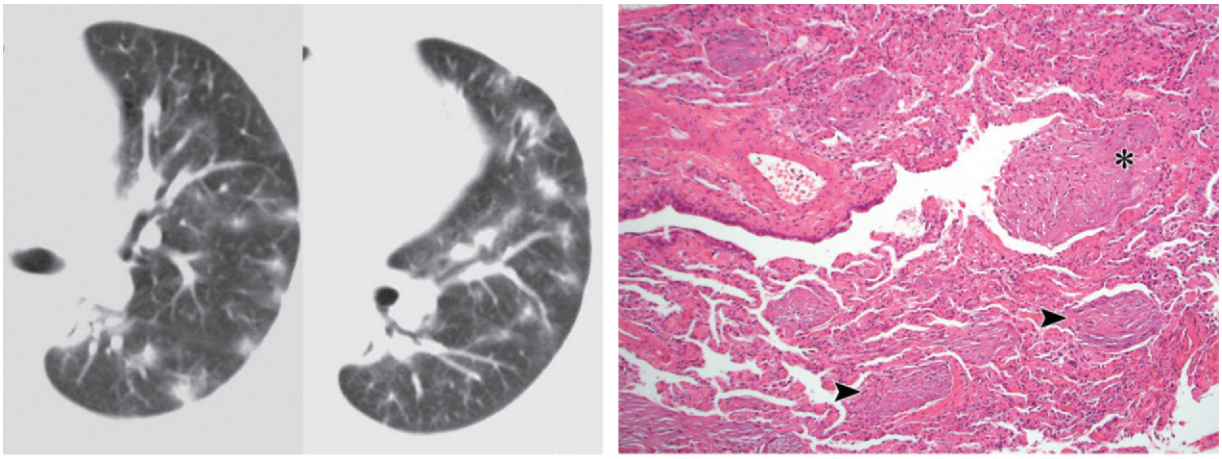

a. b.

Figure 22. Secondary OP due to systemic lupus erythematosus in a 39-year-old woman. **(a)** Axial CT images obtained through the left upper lobe (left) and left lower lobe (right) demonstrate multiple nodules primarily in the periphery of the lung. Most of the nodules are surrounded by a halo of GGO. **(b)** Photomicrograph (original magnification, ×100; H-E stain) from a transbronchial biopsy shows a plug of organizing fibroblastic tissue in an alveolar duct (*) and multiple additional plugs in the surrounding alveolar spaces (arrowheads).

can help differentiate larger nodules from other pathologic processes with similar-appearing nodules, such as parenchymal lymphoma, septic emboli, or granulomatosis with polyangiitis (Fig 20). Diffuse micronodules or tree-in-bud centrilobular nodules have been described but are uncommon (52).

Teaching Point

Differentiation of primary from secondary causes of diffuse OP often is difficult, and there is no reliable way to differentiate the two based on parenchymal findings alone (43,45,49). Small pleural effusions are more commonly seen in secondary causes of OP (49). Esophageal dilatation, soft-tissue calcifications, and bone erosions suggest an underlying connective tissue disease. Because infection is one of the most common causes of OP, a shorter duration of symptoms and underlying fever are suggestive of secondary OP (49).

After a diagnosis of OP is confirmed, potential inciting factors are removed. Patients are treated with corticosteroid therapy alone or combined with cytotoxic agents for 6–12 months (41,43,58). How corticosteroids lead to a disappearance of the well-organized fibroblastic plugs remains a mystery, although some believe that certain enzymes produced by leukocytes and fibroblasts may lead to degradation of the intraalveolar material (41). The resolution of the fibroblasts and myofibroblasts also may occur through apoptosis (39). The prognosis is good in many cases of OP, although relapses occur in 13%–58% of patients (41,43,45,49). While some studies demonstrate a higher rate of relapse in patients with secondary forms of OP-associated collagen-vascular disease (45,58), others have shown no difference in relapse rates for patients with a cryptogenic versus a secondary cause of OP (43,47). In most cases, the overall degree of lung injury usually is mild and the lung repairs itself without permanent injury (5,8,39,59,60). However, severe injury can lead to permanent damage and interstitial fibrosis.

The integrity of the epithelial and endothelial basement membranes is the key determinant of whether injured lung returns to normal or is

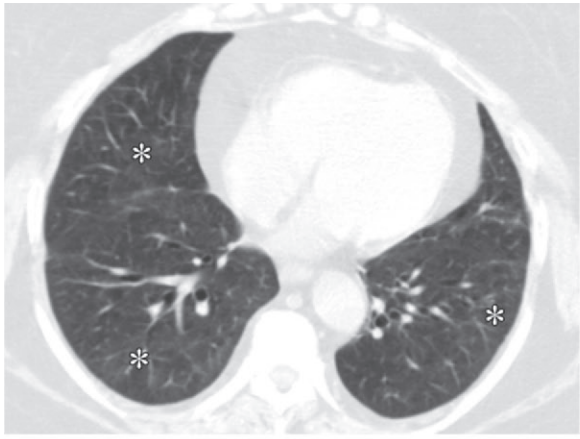

a.

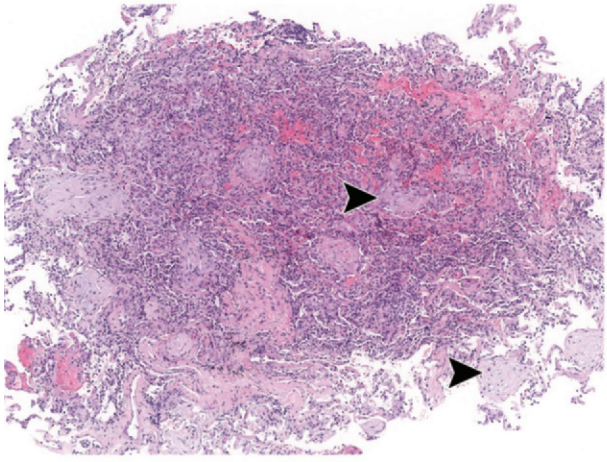

b.

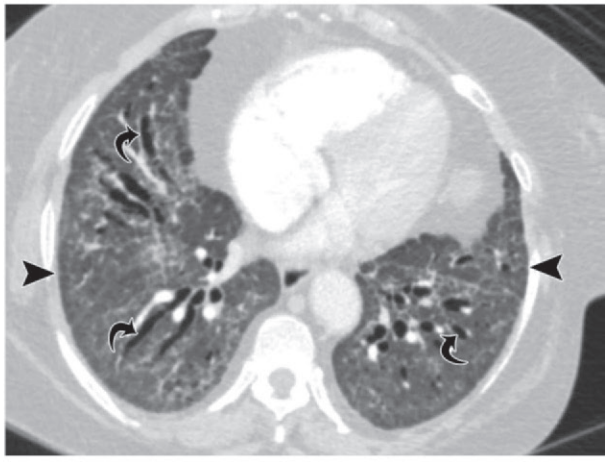

c.

Figure 23. COP in a 48-year-old woman with progressive dyspnea. **(a)** Axial CT image obtained at presentation reveals mild patchy areas of GGO in the right middle lobe and at both lung bases (*). **(b)** Photomicrograph (original magnification, ×80; H-E stain) from a transbronchial biopsy obtained at presentation shows multiple plugs of organizing fibroblastic tissue (arrowheads), findings consistent with a histologic diagnosis of OP. **(c)** Axial CT image obtained through the lung bases 3 years after **a** and **b** reveals extensive mid- and lower-lobe GGO with reticulation (arrowheads) and marked traction bronchiectasis (arrows), findings consistent with fibrosis. The imaging pattern is suggestive of nonspecific interstitial pneumonia (NSIP).

replaced by fixed fibrous tissue (6). If the integrity of the basement membranes is lost through injury, then the affected alveoli collapse, their basement membranes fuse, and fibroblast activation persists. This is a self-reinforcing process that results in the formation of organizing fibroblastic tissue with progression to fixed fibrosis (4–8,11,12). Time is required for organizing fibroblastic tissue to evolve to fibrous tissue. Although lung biopsy is useful for identification of organizing fibroblastic tissue as well as fibrosis, the biopsy sample represents the lung at a single point in time, and the progression from organization to fibrosis is best documented with imaging studies performed at intervals.

The fibrosis associated with OP is well depicted at CT and often manifests as areas of peribronchial and peribronchiolar GGO or perilobular thickening with traction bronchiectasis and reticulation in areas of injured lung (Fig 23) (50). These areas of fibrosis may be most conspicuous after resolution of the consolidation (Fig 24). In some instances, the residual fibrosis is lower-lobe predominant, peribronchial in distribution, and demonstrates subpleural sparing, findings commonly associated with an NSIP pattern (Figs 23, 24) (61,62).

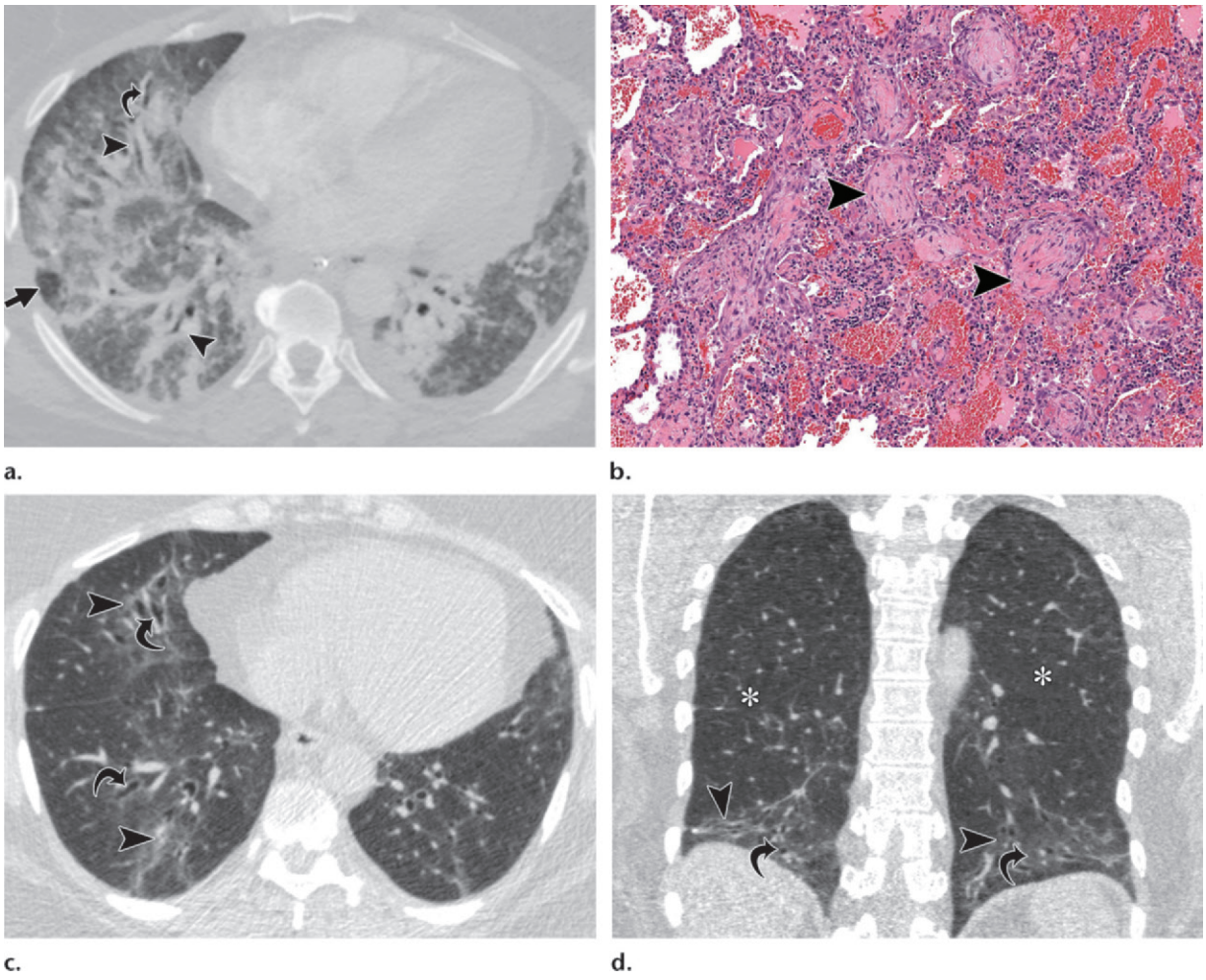

Figure 24. OP in a 39-year-old woman with rheumatoid arthritis and rapid progression of dyspnea. **(a)** Axial CT image obtained at presentation just above the level of the diaphragm reveals patchy areas of peribronchial consolidation (arrowheads) on an extensive background of GGO and very small nodules. Mild bronchiectasis (curved arrow) is seen with lobular sparing (straight arrow). **(b)** Photomicrograph (original magnification, ×100; H-E stain) from an open lung biopsy obtained at presentation shows multiple plugs of organizing fibroblastic tissue within the alveolar spaces (arrowheads), findings consistent with a histologic diagnosis of OP. **(c, d)** Axial **(c)** and coronal **(d)** CT images obtained 4 months after **a** show residual peribronchial GGO (arrowheads), inferior displacement of the major fissures (∗ in **d**) secondary to lower-lobe volume loss, and increasing traction bronchiectasis (arrows) in the lower lobes, findings consistent with an NSIP pattern.

Although it is unclear what percentage of patients will develop permanent fibrosis after developing OP, a recent study by Lee et al (62) demonstrated that 45% of patients with histologically proved OP progressed from a pattern of OP seen at initial imaging to a pattern of fibrotic NSIP seen at follow-up CT many months later. Although findings of fibrosis secondary to OP can be relatively stable, histologic and imaging progression can occur with repeated episodes of acute or subacute lung injury. In some instances, the initial insult can lead to rapidly progressive fibrosis over a short time frame (Fig 25) (63–65).

The relationship between OP and NSIP is not entirely understood, but OP is a common histologic finding in patients with NSIP. In an American Thoracic Society (66) study of idiopathic NSIP, OP was seen in 52% of biopsy specimens. Earlier studies by Cottin et al (67), Katzenstein and Fiorelli (68), and Nagai et al (69) demonstrated areas of OP associated with NSIP. Given that some patients with OP show progression to a

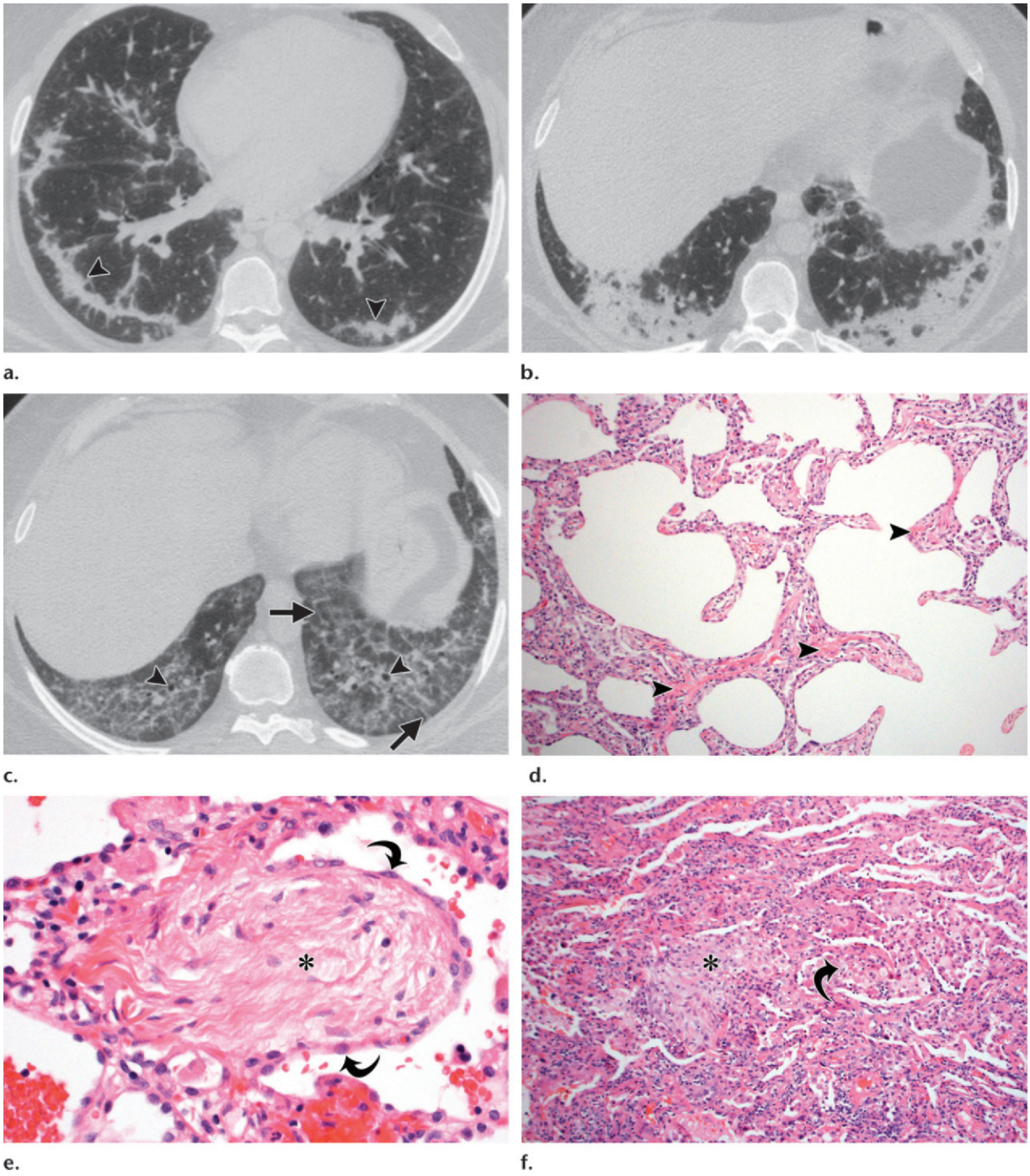

Figure 25. OP evolving into NSIP in a 62-year-old man. **(a)** Axial CT image obtained just above the diaphragm demonstrates a bandlike opacity (arrowheads) in the periphery of both lower lobes with sparing of the absolute periphery. **(b)** Axial CT image through the lower lobes obtained at the same time as **a** demonstrates more extensive consolidation. **(c)** Axial CT image obtained 9 weeks after **a** and **b** reveals widespread GGO with superimposed reticulation and traction bronchiectasis (arrowheads). Multiple septal lines are noted in the left lung (arrows). **(d)** Photomicrograph (original magnification, ×100; H-E stain) from a biopsy obtained 2 weeks after **c** shows widened alveolar walls due to loose organizing fibroblastic tissue as well as hyalinized fibrous tissue (arrowheads). In the overall biopsy, the degree of fibrosis was sufficient for the histologic diagnosis of NSIP. **(e)** Photomicrograph (original magnification, ×400; H-E stain) shows a plug (*) that has progressed from organizing fibroblastic tissue to hyalinized fibrous tissue. The alveolar epithelial cells (pneumocytes) have epithelialized the surface of the plug (arrows), which is partially incorporated into the alveolar wall. **(f)** Photomicrograph (original magnification, ×100; H-E stain) shows a zone of more recent damage and repair than in photomicrographs **d** and **e,** with a plug of organizing fibroblastic tissue in an alveolar space (*), foamy macrophages in airspaces (arrow), and mild chronic interstitial inflammation. The open lung biopsy from this patient highlights that tissue damage, repair, and fibrosis in the lung is not a sequential process but can be seen concurrently, particularly if injury is ongoing.

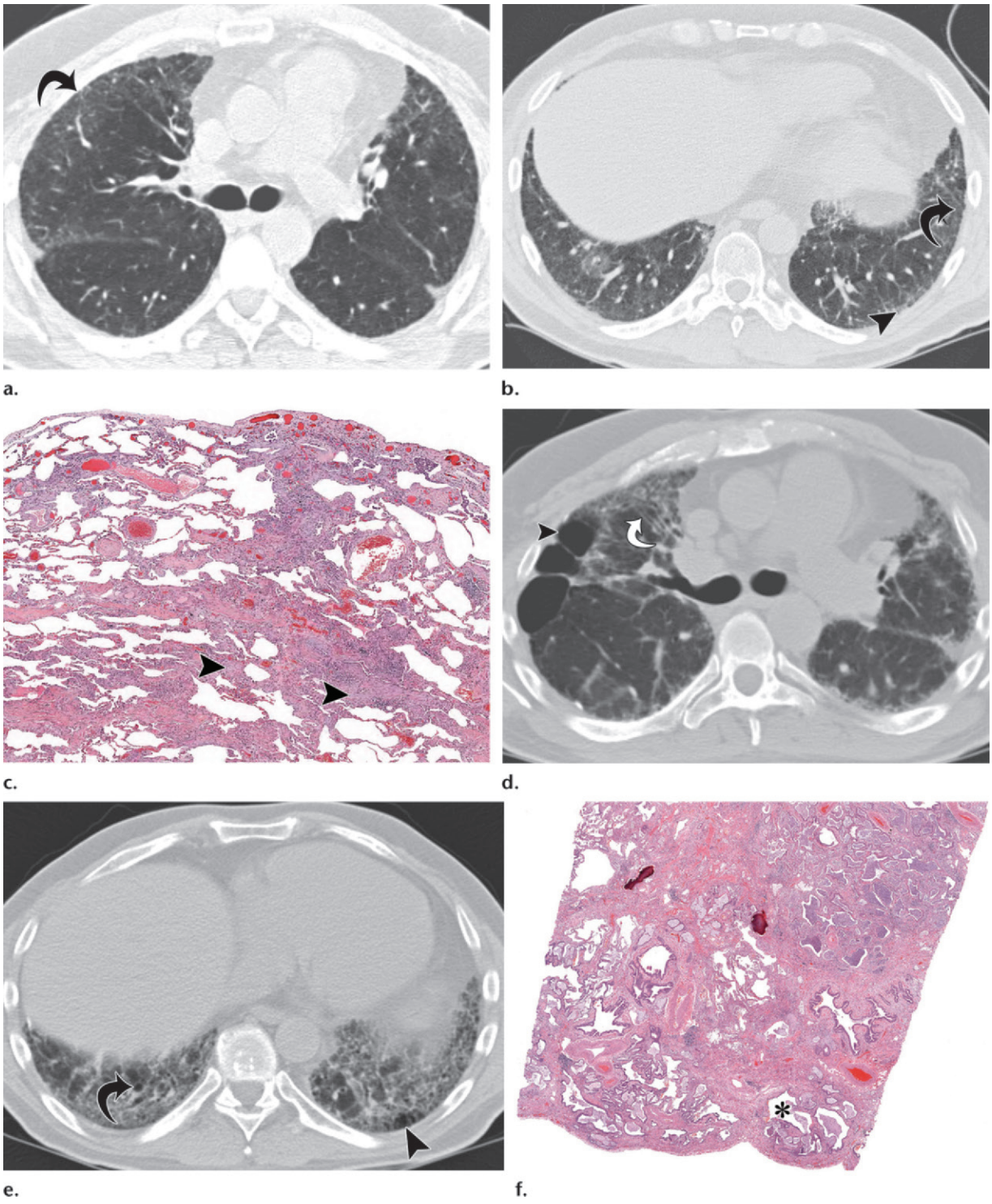

Figure 26. COP in a 56-year-old man with progressive dyspnea over 6 years. **(a, b)** Axial CT images through the carina **(a)** and lower lobes **(b)** at the time of presentation reveal predominant peripheral GGO (arrow in **a** and **b**) with mild early reticulation (arrowhead in **b**). **(c)** Photomicrograph (original magnification, ×50; H-E stain) from open lung biopsy obtained at the time of presentation shows organizing fibroblastic tissue within the airspaces and partially incorporated into the alveolar walls (arrowheads), findings consistent with the histologic diagnosis of OP. The OP is associated with patchy interstitial fibrosis consistent with the histologic diagnosis of NSIP. **(d, e)** Axial CT images obtained 6 years after **a** and **b** reveal increasing mid- and lower-lung GGO and reticulation with the development of numerous subpleural cysts (arrowhead in **d** and **e**) and traction bronchiectasis (arrow in **d** and **e**). Pulmonary function tests at this time revealed severe restrictive physiology suggesting fibrosis. **(f)** Photomicrograph (original magnification, ×13; H-E stain) of the explanted lung tissue shows diffuse interstitial fibrosis. A single secondary lobule shows partial collapse (*). However, overall the secondary lobules show variable remodeling but lack collapse as well as lack fibroblast foci, findings that do not support a histologic diagnosis of UIP.

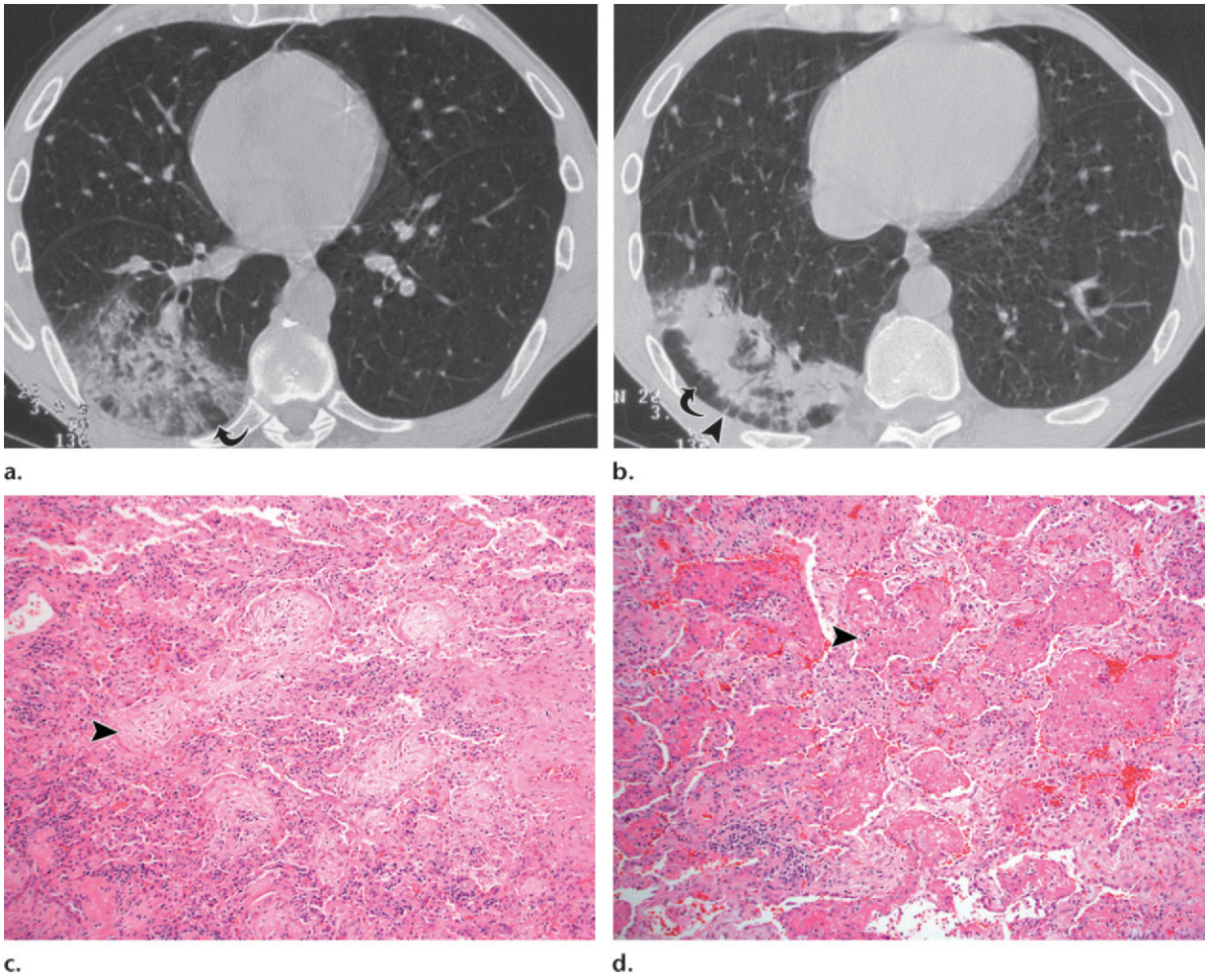

Figure 27. AFOP in a 62-year-old man. **(a)** Axial CT image at the level of the right lower-lobe segmental bronchi reveals consolidation of the lateral and posterior basal segments with lobular sparing (arrow). **(b)** Axial CT image through a more caudal portion of the chest demonstrates peripheral sparing (arrow) with multiple septal lines (arrowhead). These findings are consistent with the typical description of focal OP. **(c, d)** Photomicrographs (original magnification, ×100; H-E stain) show plugs of organizing fibroblastic tissue (arrowhead in **c**) and amorphous fibrin (arrowhead in **d**) in the alveolar spaces.

pattern of NSIP at imaging and histologic analysis, one can suggest that NSIP is a sequela of OP in some instances (Figs 25, 26). However, this remains a controversial topic.

Acute Fibrinous and Organizing Pneumonia

Acute fibrinous and organizing pneumonia (AFOP) has been described as a histologic pattern of lung injury associated with either an acute or subacute clinical presentation similar to DAD and OP. AFOP is characterized histologically by fibrin "balls" and OP within the alveolar spaces and does not meet the criteria for either DAD or OP (24). Like DAD and OP, numerous causes have been implicated, including infection, collagen-vascular disease, drug toxicity, and toxic inhalation (24,70–74). The largest study of patients with AFOP involved a series of 17 patients, nine of whom had a fulminant clinical course with rapid progression to death similar to that of DAD. The remaining patients had a subclinical course with recovery similar to that of OP (24). The clinical course and radiologic findings mirror one another as those with rapidly progressive disease have imaging findings similar to DAD with diffuse but basilar-dependent consolidation and GGO (24,75), while patients with a more subacute course have imaging findings that are indistinguishable from OP and can encompass both focal (Fig 27) and diffuse (Fig 28) parenchymal abnormality (24,72,76,77). Similar

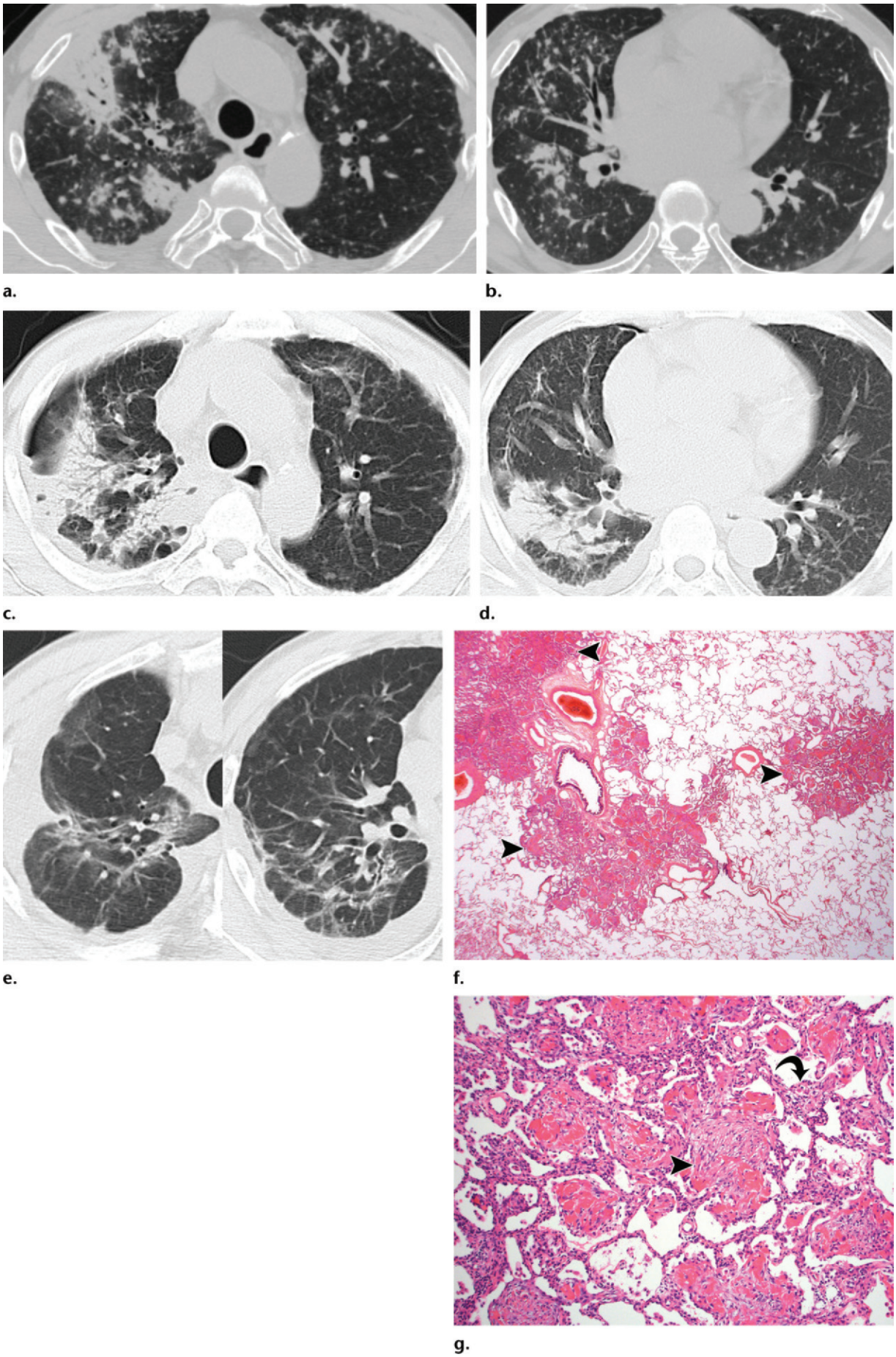
a.
b.
c.
d.
e.
f.
g.

to both DAD and OP, AFOP can lead to parenchymal fibrosis (Fig 28).

Teaching Point

DAD and OP are nonspecific reactions to lung injury and form the bookends of a spectrum from acute to subacute lung injury. Given the similarity of AFOP to the clinical presentation, clinical associations, histology, and clinical outcome of DAD and OP, the utility of the category AFOP in the spectrum of acute to subacute lung injury is unclear, and the ability to histologically reliably separate the category of AFOP from DAD and OP is unknown.

Conclusion

Organization is a common and nearly universal response to lung injury. Although there is a tendency to divide the types of organization into distinct entities, the underlying injury to the epithelial basement membrane is a uniting factor seen in both DAD and OP. The histologic and radiologic findings of these entities depend on the degree of injury and the subsequent healing response. Although lung organization can heal without permanent injury, patients with both DAD and OP can develop fibrosis. When this fibrosis due to organization progresses, other histologic and imaging patterns, such as those seen with NSIP, can develop, suggesting that organization may be a pathway to other patterns of fibrosis.

References

1. Pavelka M, Roth J. Functional ultrastructure: atlas of tissue biology and pathology. New York, NY: Springer-Verlag, 2005;225.</bok>
2. Weibel ER. Morphological basis of alveolar-capillary gas exchange. Physiol Rev 1973;53(2):419–495.
3. Katzenstein AL. Katzenstein and Askin's surgical pathology of non-neoplastic lung disease. 4th ed. Philadelphia, Pa: Saunders Elsevier, 2006;18.
4. Auerbach SH, Mims OM, Goodpasture EW. Pulmonary fibrosis secondary to pneumonia. Am J Pathol 1952;28(1):69–87.
5. Basset F, Ferrans VJ, Soler P, Takemura T, Fukuda Y, Crystal RG. Intraluminal fibrosis in interstitial lung disorders. Am J Pathol 1986;122(3):443–461.
6. Strieter RM, Mehrad B. New mechanisms of pulmonary fibrosis. Chest 2009;136(5):1364–1370.
7. Wallace WA, Fitch PM, Simpson AJ, Howie SE. Inflammation-associated remodelling and fibrosis in the lung: a process and an end point. Int J Exp Pathol 2007;88(2):103–110.
8. Myers JL, Katzenstein AL. Ultrastructural evidence of alveolar epithelial injury in idiopathic bronchiolitis obliterans-organizing pneumonia. Am J Pathol 1988;132(1):102–109.
9. Phan SH. Biology of fibroblasts and myofibroblasts. Proc Am Thorac Soc 2008;5(3):334–337.
10. Galvin JR, Frazier AA, Franks TJ. Collaborative radiologic and histopathologic assessment of fibrotic lung disease. Radiology 2010;255(3):692–706.
11. Fukuda Y, Ishizaki M, Masuda Y, Kimura G, Kawanami O, Masugi Y. The role of intraalveolar fibrosis in the process of pulmonary structural remodeling in patients with diffuse alveolar damage. Am J Pathol 1987;126(1):171–182.
12. Peyrol S, Cordier JF, Grimaud JA. Intra-alveolar fibrosis of idiopathic bronchiolitis obliterans-organizing pneumonia: cell-matrix patterns. Am J Pathol 1990;137(1):155–170.
13. Mukhopadhyay S, Parambil JG. Acute interstitial pneumonia (AIP): relationship to Hamman-Rich syndrome, diffuse alveolar damage (DAD), and acute respiratory distress syndrome (ARDS). Semin Respir Crit Care Med 2012;33(5):476–485.
14. Castro CY. ARDS and diffuse alveolar damage: a pathologist's perspective. Semin Thorac Cardiovasc Surg 2006;18(1):13–19.
15. Burkhardt A. Alveolitis and collapse in the pathogenesis of pulmonary fibrosis. Am Rev Respir Dis 1989;140(2):513–524.
16. Chapman HA. Epithelial-mesenchymal interactions in pulmonary fibrosis. Annu Rev Physiol 2011;73:413–435.
17. Katzenstein AL. Pathogenesis of "fibrosis" in interstitial pneumonia: an electron microscopic study. Hum Pathol 1985;16(10):1015–1024.
18. Ferguson EC, Berkowitz EA. Lung CT. II. The interstitial pneumonias: clinical, histologic, and CT manifestations. AJR Am J Roentgenol 2012;199(4):W464–W476.
19. Rouby JJ, Puybasset L, Nieszkowska A, Lu Q. Acute respiratory distress syndrome: lessons from computed tomography of the whole lung. Crit Care Med 2003;31(4 suppl):S285–S295.
20. Desai SR, Wells AU, Rubens MB, Evans TW, Hansell DM. Acute respiratory distress syndrome: CT abnormalities at long-term follow-up. Radiology 1999;210(1):29–35.
21. Lynch DA, Travis WD, Müller NL, et al. Idiopathic interstitial pneumonias: CT features. Radiology 2005;236(1):10–21.

◀ **Figure 28.** AFOP in a 52-year-old man with a cough and fever. **(a, b)** Axial CT images obtained at presentation show numerous 2–3-mm nodules and focal areas of peripheral and peribronchial consolidation more numerous in the right lung. **(c, d)** Axial CT images obtained 1 month after the initial study and 2 weeks after an open lung biopsy demonstrate crescent-shaped areas of peribronchial consolidation in the right lung and clearing of the small nodules seen in **a** and **b**. **(e)** Axial CT images obtained 6 weeks after **a** and **b** demonstrate further clearing, with residual peribronchial fibrosis and distortion. **(f, g)** Photomicrographs (original magnification, ×12.5; H-E stain) show airway-centered nodules (arrowheads in **f**) that are composed of organizing fibroblastic tissue admixed with fibrin (arrowhead in **g**) within the alveolar spaces. The alveolar walls are focally widened by interstitial organizing fibroblastic tissue, mild infiltrates of chronic inflammatory cells, and type 2 pneumocyte hyperplasia (arrow in **g**).

22. Ichikado K, Suga M, Gushima Y, et al. Hyperoxia-induced diffuse alveolar damage in pigs: correlation between thin-section CT and histopathologic findings. Radiology 2000;216(2):531–538.
23. Ichikado K, Suga M, Müller NL, et al. Acute interstitial pneumonia: comparison of high-resolution computed tomography findings between survivors and nonsurvivors. Am J Respir Crit Care Med 2002; 165(11):1551–1556.
24. Beasley MB, Franks TJ, Galvin JR, Gochuico B, Travis WD. Acute fibrinous and organizing pneumonia: a histological pattern of lung injury and possible variant of diffuse alveolar damage. Arch Pathol Lab Med 2002;126(9):1064–1070.
25. Ichikado K, Suga M, Muranaka H, et al. Prediction of prognosis for acute respiratory distress syndrome with thin-section CT: validation in 44 cases. Radiology 2006;238(1):321–329.
26. Joynt GM, Antonio GE, Lam P, et al. Late-stage adult respiratory distress syndrome caused by severe acute respiratory syndrome: abnormal findings at thin-section CT. Radiology 2004;230(2):339–346.
27. Masclans JR, Roca O, Muñoz X, et al. Quality of life, pulmonary function, and tomographic scan abnormalities after ARDS. Chest 2011;139(6): 1340–1346.
28. Ng CK, Chan JW, Kwan TL, et al. Six month radiological and physiological outcomes in severe acute respiratory syndrome (SARS) survivors. Thorax 2004;59(10):889–891.
29. Nöbauer-Huhmann IM, Eibenberger K, Schaefer-Prokop C, et al. Changes in lung parenchyma after acute respiratory distress syndrome (ARDS): assessment with high-resolution computed tomography. Eur Radiol 2001;11(12):2436–2443.
30. Wilcox ME, Patsios D, Murphy G, et al. Radiologic outcomes at 5 years after severe ARDS. Chest 2013;143(4):920–926.
31. Gosink BB, Friedman PJ, Liebow AA. Bronchiolitis obliterans: roentgenologic-pathologic correlation. Am J Roentgenol Radium Ther Nucl Med 1973;117 (4):816–832.
32. Katzenstein AL, Zisman DA, Litzky LA, Nguyen BT, Kotloff RM. Usual interstitial pneumonia: histologic study of biopsy and explant specimens. Am J Surg Pathol 2002;26(12):1567–1577.
33. Collard HR, Moore BB, Flaherty KR, et al. Acute exacerbations of idiopathic pulmonary fibrosis. Am J Respir Crit Care Med 2007;176(7):636–643.
34. Kim DS, Park JH, Park BK, Lee JS, Nicholson AG, Colby T. Acute exacerbation of idiopathic pulmonary fibrosis: frequency and clinical features. Eur Respir J 2006;27(1):143–150.
35. Kondoh Y, Taniguchi H, Kawabata Y, Yokoi T, Suzuki K, Takagi K. Acute exacerbation in idiopathic pulmonary fibrosis: analysis of clinical and pathologic findings in three cases. Chest 1993;103 (6):1808–1812.
36. Parambil JG, Myers JL, Ryu JH. Histopathologic features and outcome of patients with acute exacerbation of idiopathic pulmonary fibrosis undergoing surgical lung biopsy. Chest 2005;128(5):3310–3315.
37. Silva CIS, Müller NL, Fujimoto K, et al. Acute exacerbation of chronic interstitial pneumonia: high-resolution computed tomography and pathologic findings. J Thorac Imaging 2007;22(3):221–229.
38. Symmers D, Hoffman AM. The increasing incidence of organizing pneumonia. JAMA 1923;81(4): 297–298.
39. Cordier JF. Cryptogenic organising pneumonia. Eur Respir J 2006;28(2):422–446.
40. Drakopanagiotakis F, Polychronopoulos V, Judson MA. Organizing pneumonia. Am J Med Sci 2008; 335(1):34–39.
41. Cordier JF. Organising pneumonia. Thorax 2000; 55(4):318–328.
42. Cordier JF. Cryptogenic organizing pneumonia. Clin Chest Med 2004;25(4):727–738, vi–vii.
43. Drakopanagiotakis F, Paschalaki K, Abu-Hijleh M, et al. Cryptogenic and secondary organizing pneumonia: clinical presentation, radiographic findings, treatment response, and prognosis. Chest 2011;139 (4):893–900.
44. Pardo J, Panizo A, Sola I, Queipo F, Martinez-Peñuela A, Carias R. Prognostic value of clinical, morphologic, and immunohistochemical factors in patients with bronchiolitis obliterans-organizing pneumonia. Hum Pathol 2013;44(5):718–724.
45. Lohr RH, Boland BJ, Douglas WW, et al. Organizing pneumonia: features and prognosis of cryptogenic, secondary, and focal variants. Arch Intern Med 1997;157(12):1323–1329.
46. Cazzato S, Zompatori M, Baruzzi G, et al. Bronchiolitis obliterans-organizing pneumonia: an Italian experience. Respir Med 2000;94(7):702–708.
47. Oymak FS, Demirbaş HM, Mavili E, et al. Bronchiolitis obliterans organizing pneumonia: clinical and roentgenological features in 26 cases. Respiration 2005;72(3):254–262.
48. Romero S, Barroso E, Rodriguez-Paniagua M, Aranda FI. Organizing pneumonia adjacent to lung cancer: frequency and clinico-pathologic features. Lung Cancer 2002;35(2):195–201.
49. Vasu TS, Cavallazzi R, Hirani A, Sharma D, Weibel SB, Kane GC. Clinical and radiologic distinctions between secondary bronchiolitis obliterans organizing pneumonia and cryptogenic organizing pneumonia. Respir Care 2009;54(8):1028–1032.

50. Ujita M, Renzoni EA, Veeraraghavan S, Wells AU, Hansell DM. Organizing pneumonia: perilobular pattern at thin-section CT. Radiology 2004;232(3): 757–761.
51. Epler GR. Bronchiolitis obliterans organizing pneumonia. Arch Intern Med 2001;161(2):158–164.
52. Roberton BJ, Hansell DM. Organizing pneumonia: a kaleidoscope of concepts and morphologies. Eur Radiol 2011;21(11):2244–2254.
53. Murata K, Khan A, Herman PG. Pulmonary parenchymal disease: evaluation with high-resolution CT. Radiology 1989;170(3 Pt 1):629–635.
54. Jeong YJ, Kim KI, Seo IJ, et al. Eosinophilic lung diseases: a clinical, radiologic, and pathologic overview. RadioGraphics 2007;27(3):617–637, discussion 637–639.
55. Marchiori E, Zanetti G, Meirelles GSP, Escuissato DL, Souza AS Jr, Hochhegger B. The reversed halo sign on high-resolution CT in infectious and noninfectious pulmonary diseases. AJR Am J Roentgenol 2011;197(1):W69–W75.
56. Kim SJ, Lee KS, Ryu YH, et al. Reversed halo sign on high-resolution CT of cryptogenic organizing pneumonia: diagnostic implications. AJR Am J Roentgenol 2003;180(5):1251–1254.
57. Akira M, Yamamoto S, Sakatani M. Bronchiolitis obliterans organizing pneumonia manifesting as multiple large nodules or masses. AJR Am J Roentgenol 1998;170(2):291–295.
58. Yoo JW, Song JW, Jang SJ, et al. Comparison between cryptogenic organizing pneumonia and connective tissue disease-related organizing pneumonia. Rheumatology (Oxford) 2011;50(5):932–938.
59. Davison AG, Heard BE, McAllister WA, Turner-Warwick ME. Cryptogenic organizing pneumonitis. Q J Med 1983;52(207):382–394.
60. Epler GR, Colby TV, McLoud TC, Carrington CB, Gaensler EA. Bronchiolitis obliterans organizing pneumonia. N Engl J Med 1985;312(3):152–158.
61. Kligerman SJ, Groshong S, Brown KK, Lynch DA. Nonspecific interstitial pneumonia: radiologic, clinical, and pathologic considerations. RadioGraphics 2009;29(1):73–87.
62. Lee JW, Lee KS, Lee HY, et al. Cryptogenic organizing pneumonia: serial high-resolution CT findings in 22 patients. AJR Am J Roentgenol 2010;195 (4):916–922.
63. Al-Ghanem S, Al-Jahdali H, Bamefleh H, Khan AN. Bronchiolitis obliterans organizing pneumonia: pathogenesis, clinical features, imaging and therapy review. Ann Thorac Med 2008;3(2):67–75.
64. Cohen AJ, King TE Jr, Downey GP. Rapidly progressive bronchiolitis obliterans with organizing pneumonia. Am J Respir Crit Care Med 1994;149 (6):1670–1675.
65. Beardsley B, Rassl D. Fibrosing organising pneumonia. J Clin Pathol 2013 Jul 6. [Epub ahead of print]
66. Travis WD, Hunninghake G, King TE Jr, et al. Idiopathic nonspecific interstitial pneumonia: report of an American Thoracic Society project. Am J Respir Crit Care Med 2008;177(12):1338–1347.
67. Cottin V, Donsbeck AV, Revel D, Loire R, Cordier JF. Nonspecific interstitial pneumonia: individualization of a clinicopathologic entity in a series of 12 patients. Am J Respir Crit Care Med 1998;158 (4):1286–1293.
68. Katzenstein AL, Fiorelli RF. Nonspecific interstitial pneumonia/fibrosis: histologic features and clinical significance. Am J Surg Pathol 1994;18(2):136–147.
69. Nagai S, Kitaichi M, Itoh H, Nishimura K, Izumi T, Colby TV. Idiopathic nonspecific interstitial pneumonia/fibrosis: comparison with idiopathic pulmonary fibrosis and BOOP. Eur Respir J 1998;12 (5):1010–1019.
70. Hariri LP, Mino-Kenudson M, Shea B, et al. Distinct histopathology of acute onset or abrupt exacerbation of hypersensitivity pneumonitis. Hum Pathol 2012;43(5):660–668.
71. Lee SM, Park JJ, Sung SH, et al. Acute fibrinous and organizing pneumonia following hematopoietic stem cell transplantation. Korean J Intern Med 2009;24(2):156–159.
72. Valim V, Rocha RH, Couto RB, Paixao TS, Serrano EV. Acute fibrinous and organizing pneumonia and undifferentiated connective tissue disease: a case report. Case Rep Rheumatol 2012;2012:549298.
73. Papiris SA, Triantafillidou C, Kolilekas L, Markoulaki D, Manali ED. Amiodarone: review of pulmonary effects and toxicity. Drug Saf 2010;33(7): 539–558.
74. Hwang DM, Chamberlain DW, Poutanen SM, Low DE, Asa SL, Butany J. Pulmonary pathology of severe acute respiratory syndrome in Toronto. Mod Pathol 2005;18(1):1–10.
75. Prahalad S, Bohnsack JF, Maloney CG, Leslie KO. Fatal acute fibrinous and organizing pneumonia in a child with juvenile dermatomyositis. J Pediatr 2005; 146(2):289–292.
76. Kobayashi H, Sugimoto C, Kanoh S, Motoyoshi K, Aida S. Acute fibrinous and organizing pneumonia: initial presentation as a solitary nodule. J Thorac Imaging 2005;20(4):291–293.
77. Tzouvelekis A, Koutsopoulos A, Oikonomou A, et al. Acute fibrinous and organising pneumonia: a case report and review of the literature. J Med Case Reports 2009;3:74.

RadioGraphics

From the Radiologic Pathology Archives
Organization and Fibrosis as a Response to Lung Injury in Diffuse Alveolar Damage, Organizing Pneumonia, and Acute Fibrinous and Organizing Pneumonia

Seth J. Kligerman, MD • Teri J. Franks, MD • Jeffrey R. Galvin, MD

RadioGraphics 2013; 33:1951–1975 • **Published online** 10.1148/rg.337130057 • **Content Codes:** CH CT

Pages 1953

The common result of injury is that a protein-rich exudate leaks from the barrier into the alveolar space and is associated with migration of fibroblasts from the interstitium, differentiation of some fibroblasts into myofibroblasts, and formation of organizing fibroblastic tissue. The integrity of the epithelial and endothelial basement membranes is the key determinant of whether injured lung returns to normal or is replaced by fixed fibrous tissue.

Page 1957

At imaging, the acute phase of DAD manifests as relatively diffuse but patchy GGO with areas of consolidation and septal thickening (Figs 8, 9). These findings reflect a combination of airspace exudates, interstitial edema, inflammation, and alveolar collapse that usually is most pronounced in the dependent portion of the lungs (Figs. 8, 9).

Page 1961

The clinical significance of a histologic finding of OP varies. The finding may be of little clinical significance, such as in the case of focal areas of OP that surround a granuloma or malignancy (Fig 14). In addition, OP can be a minor component of diffuse lung disease such as hypersensitivity pneumonitis, eosinophilic pneumonia, or pulmonary Langerhans cell histiocytosis (3). On the other hand, the pattern may be widespread and may be the cause of the underlying clinical illness.

Page 1966

Differentiation of primary from secondary causes of diffuse OP often is difficult, and there is no reliable way to differentiate the two based on parenchymal findings alone.

Page 1973

DAD and OP are nonspecific reactions to lung injury and form the bookends of a spectrum from acute to subacute lung injury. Given the similarity of AFOP to the clinical presentation, clinical associations, histology, and clinical outcome of DAD and OP, the utility of the category AFOP in the spectrum of acute to subacute lung injury is unclear, and the ability to histologically reliably separate the category of AFOP from DAD and OP is unknown.